

Search for new phenomena in dijet events using 37 fb^{-1} of pp collision data collected at $\sqrt{s} = 13 \text{ TeV}$ with the ATLAS detector

M. Aaboud *et al.**

(ATLAS Collaboration)

(Received 28 March 2017; published 28 September 2017)

Dijet events are studied in the proton-proton collision data set recorded at $\sqrt{s} = 13 \text{ TeV}$ with the ATLAS detector at the Large Hadron Collider in 2015 and 2016, corresponding to integrated luminosities of 3.5 fb^{-1} and 33.5 fb^{-1} respectively. Invariant mass and angular distributions are compared to background predictions and no significant deviation is observed. For resonance searches, a new method for fitting the background component of the invariant mass distribution is employed. The data set is then used to set upper limits at a 95% confidence level on a range of new physics scenarios. Excited quarks with masses below 6.0 TeV are excluded, and limits are set on quantum black holes, heavy W' bosons, W^* bosons, and a range of masses and couplings in a Z' dark matter mediator model. Model-independent limits on signals with a Gaussian shape are also set, using a new approach allowing factorization of physics and detector effects. From the angular distributions, a scale of new physics in contact interaction models is excluded for scenarios with either constructive or destructive interference. These results represent a substantial improvement over those obtained previously with lower integrated luminosity.

DOI: [10.1103/PhysRevD.96.052004](https://doi.org/10.1103/PhysRevD.96.052004)

I. INTRODUCTION

The Large Hadron Collider (LHC) [1] at CERN has been colliding protons at a center-of-mass energy of $\sqrt{s} = 13 \text{ TeV}$ since 2015. With the completion of the 2016 physics run, the total integrated luminosity of run-2 data at 13 TeV now exceeds that of the total run-1 data set by more than 10 fb^{-1} . When combined with the increase in parton luminosity [2] at high energy scales, due to the raising of the center-of-mass energy from 8 to 13 TeV, this very large data set provides an exceptional opportunity to search for new phenomena.

New particles directly produced in proton-proton (pp) collisions must interact with the constituent partons of the proton and, consequently, can produce partons when they decay. Such partonic final states dominate in many models of new phenomena beyond the Standard Model (BSM) which are accessible at the LHC. The partons shower and hadronize, creating collimated jets of particles carrying approximately the four-momenta of the partons. The production rates for BSM signals decaying to two-jet (dijet) final states can be large, allowing such signals to be probed through searches for anomalous dijet production at masses constituting significant fractions of the total hadron collision energy.

In the Standard Model (SM), hadronic collision production of jet pairs primarily results from $2 \rightarrow 2$ parton scattering processes via strong interactions described by quantum chromodynamics (QCD). Particles emerge from these collisions as jets with high transverse momentum (p_T) with respect to the incoming partons. A smooth and monotonically decreasing distribution for the dijet invariant mass, m_{jj} , is predicted by QCD [3]. The presence of a new resonant state decaying to two jets may introduce an excess in this distribution, localized near the mass of this resonance. Furthermore, in QCD most dijet production occurs in the forward direction at small angles θ^* , defined as the polar angle with respect to the direction of the initial partons in the dijet center-of-mass frame,¹ due to t -channel poles in the cross sections for the dominant scattering processes. Many theories of BSM physics predict additional dijet production with a more isotropic signature, and thus a significant population of jets produced at large θ^* [3,4]. The search reported in this paper exploits these generic features of BSM signals in an analysis of the dijet mass and angular distributions. Following a model-nonspecific search for deviations from the SM in both types of distributions, limits are set on the masses of excited quarks, quantum black holes, W' and Z' bosons, and excited chiral W^* bosons, on contact interactions scales, and on generic Gaussian-shaped signal production.

Results from prior investigations of dijet distributions with lower-energy hadron collisions at the $S\bar{p}pS$ [5–7], the Tevatron [8,9], and the LHC at $\sqrt{s} = 7\text{--}8 \text{ TeV}$ [10–21]

*Full author list given at the end of the article.

Published by the American Physical Society under the terms of the [Creative Commons Attribution 4.0 International license](https://creativecommons.org/licenses/by/4.0/). Further distribution of this work must maintain attribution to the author(s) and the published article's title, journal citation, and DOI.

¹Since, experimentally, the two partons cannot be distinguished, θ^* is always taken between 0 and $\pi/2$.

were found to be in agreement with QCD predictions. Recent searches at 13 TeV [22–24] included extensions of the analysis to di-*b*-jet final states [25] and to lower masses [24,26], and observed no significant deviations from the Standard Model. This paper presents an analysis of the full 2015 and 2016 data sets recorded by the ATLAS detector at the LHC, corresponding to 37.0 fb^{-1} of pp collision data at $\sqrt{s} = 13 \text{ TeV}$.

II. ATLAS DETECTOR

The ATLAS experiment [27,28] at the LHC is a multipurpose particle detector with a forward-backward symmetric cylindrical geometry with layers of tracking, calorimeter, and muon detectors over nearly the entire solid angle around the pp collision point.² The directions and energies of high- p_T hadronic jets are measured using silicon tracking detectors and a transition radiation straw-tube tracker, hadronic and electromagnetic calorimeters, and a muon spectrometer. Hadronic energy measurements are provided by a calorimeter with scintillator active layers and steel absorber material for the pseudorapidity range $|\eta| < 1.7$, while electromagnetic (EM) energy measurements are provided by a calorimeter with liquid argon (LAr) active material and lead absorber material covering the pseudorapidity range $|\eta| < 3.2$. The endcap and forward regions, extending up to $|\eta| = 4.9$, are instrumented with LAr calorimeters for both EM and hadronic energy measurements. The lower-level trigger is implemented in hardware and uses a subset of the detector information to reduce the accepted rate to 100 kHz. This is followed by a software-based high-level trigger that reduces the rate of events recorded to 1 kHz [29].

III. EVENT SELECTION

Groups of contiguous calorimeter cells (topological clusters) are formed based on the significance of local energy deposits over calorimeter noise [30,31]. Topological clusters are grouped into jets using the anti- k_r algorithm [32,33] with radius parameter $R = 0.4$. Jet four-momenta are computed by summing over the topological clusters that constitute each jet, treating the energy of each cluster as resulting from a four-momentum with zero mass. Jets with p_T above 20 GeV are reconstructed with an efficiency of nearly 100%. Jet calibrations derived from simulation are used to correct the jet energies and directions to those of particle-level jets from the hard-scatter interaction clustered

²ATLAS uses a right-handed coordinate system with its origin at the nominal interaction point (IP) in the center of the detector and the z axis along the beam line. The x axis points from the IP to the center of the LHC ring, and the y -axis points upwards. Cylindrical coordinates (r, ϕ) are used in the transverse plane, ϕ being the azimuthal angle around the z axis. The pseudorapidity is defined in terms of the polar angle θ as $\eta = -\ln \tan(\theta/2)$. It is equivalent to the rapidity for massless particles.

with the same algorithm and parameters.³ This calibration procedure [35–40] is followed by a residual calibration accounting for the differences between data and simulation, beginning with a correction to the relative response for forward jets ($|\eta| > 0.8$) with respect to central jets ($|\eta| < 0.8$). Using this method and other *in situ* techniques where a jet to be calibrated is balanced against a well-calibrated reference object [41,42], analysis of jet data at 13 TeV corrects the jet response and contributes to the uncertainty estimates up to jet p_T values of 2.3 TeV, beyond which the calibration is frozen.

The total jet energy scale uncertainty is 1% for central jets with p_T of 500 GeV and grows to 3% for jets with p_T of 2 TeV, at which point, due to the limited size of the event sample available for the *in situ* studies, an uncertainty is derived from alternative methods using the single-particle response measurements described in Ref. [43]. Uncertainty in the jet energy resolution has a negligible impact on the analysis. The dijet mass resolution is 2.4% and 2.0% for dijet masses of 2 and 5 TeV, respectively, derived at 13 TeV from the simulation of QCD processes as in Ref. [23].

Collision events are recorded using a trigger that requires at least one jet reconstructed by the high-level trigger with a p_T greater than 380 GeV, the lowest- p_T single-jet trigger that saves all events that activate it. Events containing at least two jets are selected for offline analysis if the p_T of the leading (subleading) jet is greater than 440 (60) GeV. This requirement ensures a trigger efficiency of at least 99.5% for collisions that enter into the analysis. Events are discarded from the search if any jets with $p_T > 60 \text{ GeV}$ are compatible with noncollision background or calorimeter noise [44].

IV. MONTE CARLO SIMULATION

Monte Carlo (MC) events from multijet production described by QCD are generated with PYTHIA 8.186 [45] using the A14 [46] set of tuned parameters for the underlying event and the leading-order NNPDF2.3 [47] parton distribution functions (PDFs). The renormalization and factorization scales are set to the average p_T of the two leading anti- k_r , $R = 0.4$ truth jets. Detector effects are simulated using GEANT4 [48] within the ATLAS software infrastructure [49]. The same software used to reconstruct data is also used to reconstruct simulated events. The simulated events are used to provide a background estimate for the dijet angular distributions, to test the data-based background estimate used for the m_{jj} distribution, and to provide qualitative comparisons to kinematic distributions in data.

³The “particle level” jets are built from stable particles defined by having a proper mean decay length of $c\tau > 10 \text{ mm}$. Particles from interactions other than the hard scattering, as well as muons and neutrinos, are not included in this definition. More information about the particle definition can be found in Ref. [34].

PYTHIA calculations use matrix elements that are at leading order in the QCD coupling constant, with simulation of higher-order contributions partially covered by the parton shower modeling. They also include modeling of hadronization effects. The distributions of events predicted by PYTHIA are reweighted to next-to-leading-order (NLO) predictions of NLOJET++ [50–52] using mass- and angle-dependent correction factors defined as in Ref. [21]. The correction factors modify the shape of the angular distributions at the level of 15% at high values of m_{jj} and low rapidity separation between the leading and subleading jets. The correction is 5% or less for the highest values of rapidity separation. The PYTHIA predictions also omit electroweak effects. These are included as additional mass- and angle-dependent correction factors [53] that differ from unity by up to 3% in the $m_{jj} > 3.4$ TeV region. The PYTHIA distributions corrected for NLO and electroweak effects are compared to the angular and m_{jj} distributions in data and are found to be in good agreement within experimental uncertainties.

Signal samples are generated as described in Sec. VII for a range of benchmark models: excited quarks (q^*) [54,55], new heavy vector bosons (W' , Z') [56–58], excited chiral bosons (W^*) [59,60], quantum black holes (QBH) [61–63] and contact interactions [64,65]. After these signals are simulated, most of the samples are reconstructed using the same framework as used for QCD processes, though a small fraction of the samples employ a simplified parametrization of the detector as described in Ref. [66] for improved processing time. No difference between full simulation and this fast simulation is observed in the relevant variables for this analysis.

V. RESONANCE SEARCH

The m_{jj} distribution formed from the two leading jets in selected events is analyzed for evidence of contributions from resonant BSM phenomena. The rapidity of an outgoing parton is $y = 1/2 \ln[(E + p_z)/(E - p_z)]$, where E is its energy and p_z is the component of its momentum along the z axis. The rapidity difference $y^* = (y_1 - y_2)/2$ is defined between the two leading jets and is invariant under Lorentz boosts along the z axis. A requirement of $|y^*| < 0.6$ reduces the background from QCD processes. This nominal selection is used for the model-independent search phase, to set limits on generically shaped signals (discussed in Sec. VII), and to constrain the q^* , QBH, W' and Z' benchmark models, all of whose distributions peak at $y^* = 0$. A second signal region with a wider selection of $|y^*| < 1.2$ is also defined, optimized for signals produced at more forward angles. The W^* benchmark model, whose distribution peaks at $|y^*| > 1.0$, is constrained using this selection. Due to the requirements on y^* and p_T the selection is fully efficient only for $m_{jj} > 1.1$ TeV (1.7 TeV for the $|y^*| < 1.2$ selection). Therefore, the analysis is performed above this mass threshold. Bin widths

are chosen to approximate the m_{jj} resolution and therefore widen as the mass increases, from about 130 GeV at the lowest m_{jj} values to about 180 GeV at the highest. They differ slightly between the $|y^*| < 0.6$ and $|y^*| < 1.2$ selections as the resolution also differs.

Figure 1 shows the observed m_{jj} distribution for events passing the two y^* selections, overlaid with examples of the signals described in Sec. VII. The background estimate is illustrated by the solid red line and is derived from the sliding-window fitting method described below. The largest value of m_{jj} detected is 8.12 TeV.

Prior dijet searches found that expressions of the form

$$f(z) = p_1(1-z)^{p_2} z^{p_3} z^{p_4 \log z}, \quad (1)$$

where $z = m_{jj}/\sqrt{s}$ and the p_i are parameters, describe dijet mass distributions observed at lower collision energies. Some past searches required fewer terms in Eq. (1), such as by setting $p_4 = 0$, but more parameters are ultimately required to describe the distribution as integrated luminosity increases [23]. Searches at CDF, as well as at ATLAS and CMS at both $\sqrt{s} = 8$ and $\sqrt{s} = 13$ TeV, previously found Eq. (1) to fit the observed spectrum [8,10,15,16,19,24]. This parametrization also provides a good description of simulated QCD samples.

With increasing luminosity and the corresponding extension of the m_{jj} range and decrease in statistical uncertainties, a single global fit to the entire spectrum using Eq. (1) cannot necessarily be relied upon. Since the global fit is still viable for this analysis, it presented an opportunity to develop new methods for addressing the background estimate. For the resonance search in this paper, a new sliding-window fitting technique is used, fitting only restricted regions of the spectrum and therefore retaining more flexibility. The limited range of the sliding-window fit allows the use of a three-parameter fit function, while the global fit requires a nonzero p_4 . The sliding-window fit produces search and limit results compatible with those from the global fit used in previous analyses. The reliability of this new background fitting method in presence of a signal has also been checked. Tests performed for the full range of signal widths considered in this paper have shown good linearity between the injected and extracted signal.

The background for the invariant mass spectrum is constructed bin-by-bin by performing a likelihood fit to the data in each window and using the fit value in the central bin of the window for the background description. At the low end of the spectrum the window is compressed down depending on the number of available bins. When it is below 60% of the nominal window size, the values for the center bin and all bins below it are taken from the fit at this window. The values from the full set of windows are then joined to create the background for the full mass range. The window size is chosen to be the widest in which the three-parameter version of Eq. (1) describes the data well in

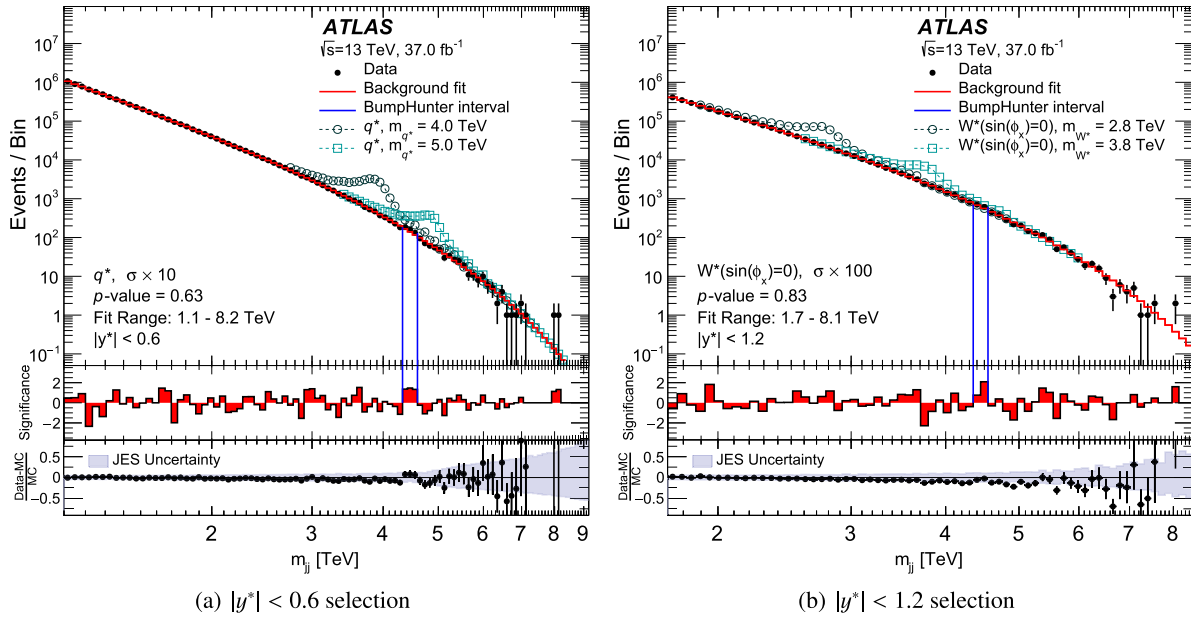


FIG. 1. The reconstructed dijet mass distribution m_{jj} (filled points) is shown for events with $p_T > 440$ (60) GeV for the leading (subleading) jet. The spectrum with $|y^*| < 0.6$ is shown in (a) for events above $m_{jj} = 1.1$ TeV while the selection with $|y^*| < 1.2$ is shown in (b) for events above $m_{jj} = 1.7$ TeV. The solid line depicts the background prediction from the sliding-window fit. Predictions for benchmark signals are normalized to a cross section large enough to make the shapes distinguishable above the data. The vertical lines indicate the most discrepant interval identified by the BUMPHUNTER algorithm, for which the p -value is stated in the figure. The middle panel shows the bin-by-bin significances of the data-fit differences, considering only statistical uncertainties. The lower panel shows the relative differences between the data and the prediction of PYTHIA 8 simulation of QCD processes, corrected for NLO and electroweak effects, and is shown purely for comparison. The shaded band denotes the experimental uncertainty in the jet energy scale calibration.

each window of the fit, considering different metrics for the fit goodness. The nominal window size covers approximately half of the total number of bins seen in Fig. 1, wide enough for all the considered benchmark signals to fit within an individual window.

The uncertainty due to the values of the parameters in Eq. (1) is estimated by repeating the sliding-window fitting procedure on pseudodata drawn via Poisson fluctuations from the nominal background prediction, that is, the fit result in data. The uncertainty in each m_{jj} bin is taken to be the root mean square of the fit results for all pseudoexperiments in that bin. To estimate an uncertainty due to the choice of background parametrization, an additional sliding-window fit using Eq. (1) with $p_4 \neq 0$ is compared to the nominal ansatz, and the average difference between the two fit results across a set of pseudodata is taken as an uncertainty. This background prediction for the m_{jj} distribution does not involve simulated collisions and is therefore not affected by uncertainties such as those due to MC modeling and statistics.

The BUMPHUNTER algorithm quantifies the statistical significance of any localized excess in the m_{jj} distribution [67,68]. The algorithm compares the binned m_{jj} distribution of the data to the fitted background estimate, considering contiguous mass intervals in all possible locations,

from a width of two bins to a width of half of the distribution. For each interval in the scan, it computes the significance of any excess found. The algorithm identifies the interval 4326–4595 GeV, indicated by the two vertical lines in Fig. 1, as the most discrepant interval in the $|y^*| < 0.6$ signal region. The global significance of this outcome is evaluated using the ensemble of possible outcomes across all intervals scanned, by applying the algorithm to pseudodata samples drawn randomly from the background fit. Without including systematic uncertainties, the probability that fluctuations of the background model would produce an excess at least as significant as the one observed in the data anywhere in the distribution (the BUMPHUNTER probability) is 0.63. Thus, there is no evidence of a localized contribution to the mass distribution from BSM phenomena. Similarly, the search in the second signal region with $|y^*| < 1.2$ shows no significant deviation from the smooth background parametrization, with the same interval identified as the most discrepant and a BUMPHUNTER probability of 0.83.

VI. ANGULAR ANALYSIS

Differences between the rapidities of two jets are invariant under Lorentz boosts along the z axis, hence the following function of the rapidity difference $2y^*$,

$$\chi = e^{2|y^*|} \sim \frac{1 + \cos \theta^*}{1 - \cos \theta^*},$$

is the same in the detector frame as in the partonic center-of-mass frame. The variable χ is constructed such that, in the limit of massless parton scattering and when only t -channel scattering contributes to the partonic cross section, the angular distribution $dN/d\chi$ is approximately independent of χ [69].

In the center-of-mass frame, the two partons have rapidity $\pm y^*$. A momentum imbalance between the two incident partons boosts the center-of-mass frame of the collision with respect to the laboratory frame along the z direction by

$$y_B = \ln(x_i/x_j) = (y_1 + y_2)/2,$$

where y_B is the rapidity of the boosted center-of-mass frame, x_i and x_j are the fractions of the proton momentum (Bjorken x) carried by each incident parton, and y_1 and y_2 are the rapidities of the outgoing partons in the detector frame. The measured shapes of the observed $dN/d\chi$ distributions differ from the parton-level distributions because the observed ones convolve the parton-level distributions with nonuniform parton momentum distributions in x_i and x_j , and also contain some admixture of non- t -channel processes. Restricting the range of the two-parton invariant mass and placing an upper bound on y_B reduces these differences.

The $dN/d\chi$ (angular) distributions of events with $|y^*| < 1.7$ and $|y_B| < 1.1$ are analyzed for contributions from BSM signals. The data with $m_{jj} < 2.5$ TeV are discarded to remove trigger inefficiencies which otherwise arise due to the loosened y^* selection compared to the resonance analysis. The data set is then analyzed by fitting to it a PYTHIA MC sample acting as an SM template as explained below. This sample is simulated as described in Sec. IV, including the aforementioned corrections. Figure 2 shows the angular distributions of the data in different m_{jj} ranges starting from 3.4 TeV, the SM prediction for the shape of the angular distributions after it is fit to data, and examples of the signals described in Sec. VII. In the statistical analysis, MC simulation is normalized to data; in Fig. 2 both the MC simulation and the data are normalized to unit integral in each m_{jj} range for clarity of display.

Theoretical uncertainties in simulations of the angular distributions from QCD processes are estimated as described in Ref. [23].⁴ The effect of varying the choice of PDF sets on the multijet prediction is estimated using NLOJET++ with three different PDF sets: CT10 [70], MSTW2008 [71] and NNPDF2.3 [47]. As the choice of

⁴Uncertainties in electroweak corrections are not yet available and so are not included.

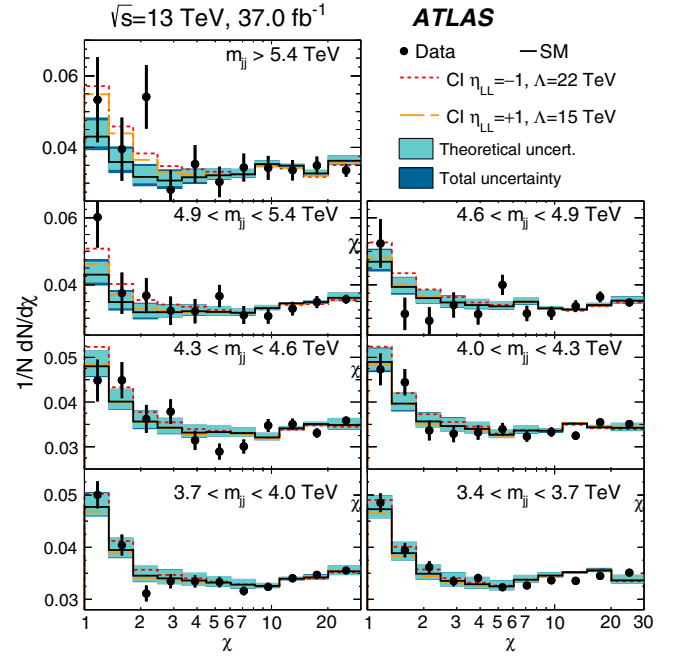


FIG. 2. Reconstructed distributions of the dijet angular variable χ in different regions of the dijet invariant mass m_{jj} for events with $|y^*| < 1.7$, $|y_B| < 1.1$, and $p_T > 440$ (60) GeV for the leading (subleading) jet. The data (points), PYTHIA predictions with NLO and electroweak corrections applied (solid lines), and examples of the contact interaction (CI) signals discussed in the text (dashed lines) are shown. The theoretical uncertainties and the total theoretical and experimental uncertainties in the predictions are displayed as shaded bands around the SM prediction. The SM background prediction and corresponding systematic uncertainty bands are extracted from the best-fit to the data. Data and predictions are normalized to unity in each m_{jj} bin.

PDF mainly affects the total cross section rather than the shape of the χ distributions, these uncertainties are negligible ($< 1\%$) in this analysis. The uncertainty due to the choice of renormalization and factorization scales is estimated using NLOJET++ by varying each one independently up and down by a factor of 2. The resulting uncertainties, taken as the variations in the normalized χ distributions, depend on both m_{jj} and χ and rise to 12% (8%) for the renormalization (factorization) scale, at the smallest χ values and high m_{jj} values. The statistical uncertainty in the simulated NLO corrections is less than 1%. The dominant experimental uncertainty in the predictions of the χ distributions is the jet energy scale uncertainty, with an impact of at most 15% at high m_{jj} values, for the raw distribution before the fit is performed. The uncertainty in the jet energy resolution has negligible impact. The theoretical uncertainties and the total uncertainties are displayed as shaded bands around the prediction in Fig. 2, where theoretical uncertainties can be seen to dominate.

The compatibility of the χ distribution in data with the SM prediction and with the BSM signals discussed in

Sec. VII is tested using a combined fit in seven coarse m_{jj} bins covering $m_{jj} > 3.4$ TeV as shown in Fig. 2. The range $m_{jj} < 3.4$ TeV provides no sensitivity to the studied benchmark models in ranges which are not yet excluded. A profile likelihood fit is performed, using as templates the $dN/d\chi$ distributions in each m_{jj} bin for data and QCD MC events. The likelihood function includes nuisance parameters corresponding to the systematic uncertainties described above, treated as correlated across bins. The MC simulation is normalized to the data separately in each m_{jj} bin, making this a shape-only comparison. All systematic uncertainties are treated as correlated in m_{jj} ; where this assumption is less secure, such as for the choice of MC event generator tune, other correlation models are tested and the differences are found to be inconsequential. The fit to the data is strongly constrained by the lowest m_{jj} bins, which have good statistical precision as well as negligible contributions from possible BSM signals, providing constraints of between 20% and 40% on the uncertainties in the higher m_{jj} bins. The CL_b , or confidence level for the background-only hypothesis, comparing data to SM predictions is 0.06. Thus no significant deviation of the data from the background-only hypothesis is observed. Limits on the production of BSM signals are set using the CL_s method [72,73], which takes the CL_b value into account and thereby avoids setting overly strong limits in light of the rather low observed p -value.

VII. BENCHMARK SIGNALS

The data are used to constrain several of the many BSM models that predict dijet excesses. Excited quarks, quantum black holes, and W' , W^* , and Z' bosons would produce peaks in the m_{jj} distribution. Contact interactions would introduce smooth changes in the high-mass tail of the m_{jj} distribution that could be detected in the analysis of the χ distributions. The signal models are simulated using the parton-level event generators indicated below, in an identical manner to QCD processes, using the same PDFs and parameters for nonperturbative effects, except where noted otherwise. The renormalization and factorization scales are set to the average p_T of the two leading jets. The efficiency for all signal models is close to unity, henceforth acceptance times efficiency is referred to as acceptance. For all models, acceptance is computed from all events which pass the analysis selection, including distribution tails caused by the sharp rise of PDFs at low Bjorken x .

If extra spatial dimensions exist, the fundamental scale of gravity could be lowered to a few TeV and the LHC could produce quantum black holes at or above this scale [4,61,62,74–77]. High-multiplicity final states from thermalizing black holes are explored at $\sqrt{s} = 13$ TeV by ATLAS in Refs. [78,79] and by CMS in Ref. [80]. This analysis explores QBH that would be produced at or above the fundamental scale of gravity M_D and decay into a few

particles rather than the high-multiplicity final states characteristic of thermalizing black holes [61–63,81]. These would appear in the m_{jj} distribution as an excess localized near the threshold mass for quantum black hole production, M_{th} . Here, production and decay to two jets is simulated using the BLACKMAX event generator [63] assuming an Arkani-Hamed–Dimopoulos–Dvali (ADD) scenario [82,83] with $M_D = M_{th}$ and a number of extra dimensions $n = 6$, as in Ref. [19]. In this model, the branching ratio to dijets is greater than 96%. The PDFs used are CTEQ6L1 [84]. The QBH signals peak slightly above their threshold values and have negligible low-mass tails. The reconstructed signal peaks have width-to-mass ratios of approximately 10%. The acceptance of the resonance search selection for quantum black holes is approximately 53% across all studied masses.

Excited quarks are predicted in models of compositeness and are a typical benchmark for quark-gluon resonances used in many past dijet searches [8,10,12,22,23]. The q^* model is simulated with PYTHIA 8.186, assuming spin-1/2 excited quarks with coupling constants the same as for SM quarks; no interference with the SM is simulated. Only the decay of the excited quark to a gluon and an up- or down-type quark is simulated; this corresponds to a branching ratio of 85%. Before parton shower effects are taken into account, the intrinsic width of the q^* signals is comparable to the detector resolution. After showering, a radiative tail is present that increases in strength for higher q^* masses, an effect augmented by the impact of PDFs decreasing towards higher masses. The resonance search selection acceptance for a q^* with a mass of 4 TeV is 58% .

Additional spin-1 W' and Z' bosons often arise in the symmetry breaking of extended gauge theories. A W' model with axial-vector SM couplings and a corresponding branching ratio to quarks of 75% is considered [85]. Events are simulated with PYTHIA 8.205 and decays are restricted to quark-antiquark pairs with all three quark-flavor doublets included. A leptophobic Z' model is also simulated, with matrix elements calculated in MADGRAPH5_AMC@NLO v2.2.3 [86] and parton showering performed in PYTHIA 8.210. The Z' model assumes axial-vector couplings to all SM quarks and to a Dirac fermion dark matter candidate. Final states with top quarks are not simulated, and the acceptance for these is assumed to be zero and is taken into account for the branching ratio and normalization of simulated data. The model considered follows a scenario [58] where the Z' branching ratio to dark matter is negligible, hence the dijet production rate and resonance width depend only on the coupling to quarks, g_q , and the mass of the resonance $m_{Z'}$. Before parton shower effects are considered, the intrinsic width of the Z' signal ranges from 0.05% of the mass of a 1.5 TeV Z' with $g_q = 0.1$ to 10% of the mass of a 3.5 TeV Z' with $g_q = 0.5$. The W' signal has an intrinsic width similar to a Z' of coupling $g_q = 0.3$ at

every mass point considered. For coupling values of $g_q = 0.6$ and above, the intrinsic width of the Z' for the mass range of interest increases to 15% and beyond, resulting in a very wide peak and in a loss of sensitivity in the resonance search, which is therefore limited to $g_q \leq 0.5$. No interference with the SM is simulated for either the W' or the Z' model. The resonance search selection acceptance for a mass of 3 TeV is 40% for the W' model and 47% for the Z' model with $g_q = 0.2$. Because of the large radiative tails of the W' signals, the acceptance for this model increases to a maximum at approximately 2.5 TeV and decreases to values smaller than 20% for masses above 6.0 TeV.

An excited W^* boson is generated through a simplified model [87] in the CalcHEP 3.6 event generator [88], in combination with the NNPDF2.3 NLO PDF set and PYTHIA 8.210 for the simulation of nonperturbative effects. The mixing angle in this model (ϕ_X) is set to zero, producing leptophobic decays of the W^* that are limited to all SM quarks. The angular distribution of the W^* differs from that of the other signals under study, peaking at y^* values above 1. Therefore, this benchmark model is constrained using the alternative signal region with $|y^*| < 1.2$. The acceptance for the leptophobic W^* signal with this selection increases from 33% around 2 TeV to nearly 60% for the highest masses examined.

Results are also provided as limits on the cross section times acceptance times branching ratio to two jets, $\sigma \times A \times \text{BR}$, of a hypothetical signal modeled as a Gaussian peak in the particle-level m_{jj} distribution. When limits are set on Gaussian signal models that can contribute to the reconstructed m_{jj} spectrum (e.g. as in Ref. [19]), the description of the corresponding distribution folds together the actual physical signal and detector effects (acceptance and resolution). Here a model is defined at particle level, within a fiducial region. This model is then folded with the effects of the detector response, described through an MC-based transfer matrix that relates the particle level and reconstructed observables. The transfer matrix accounts for bin-to-bin migrations due to resolution effects, as well as for the fractions of events passing the selection only at particle or reconstruction level. In order to avoid large simulation-based extrapolations, the fiducial selection at particle level matches the one applied at reconstruction level. Limits on a given signal model can be interpreted from the phenomenological point of view at particle level, without need for further information about the detector response.

For sufficiently narrow resonances, these results may be used to set limits in BSM models beyond those considered explicitly in this paper. The predicted signals should be compared at particle level, after applying the resonance selection, with the limit that corresponds most closely to the width of the Gaussian contribution predicted by the model. Since a Gaussian signal shape is assumed in determining the limits, any long tails in the m_{jj} distribution should not

be included in the model under study. A procedure similar to the one detailed in Appendix A.1 of Ref. [19] can be followed, after applying the nonperturbative corrections and performing the fiducial selection at particle level, without applying any further detector smearing as it is already accounted for in the folding procedure.

The folding procedure applied for the various signal samples discussed above, using transfer matrices based on either the same or different samples, yields reconstructed distributions compatible with the ones from full simulation. The limits on narrow signals at particle level, folded with the detector effects, are similar to the ones obtained for a Gaussian signal at reconstruction level having a width equal to the one expected from detector resolution.⁵ For resonance widths comparable to the resolution, differences up to about 20% are observed between the results of the two limit-setting approaches. The folding method yields results at particle level, accounting also for the mass dependence of the resolution within the range of the resonance, hence its relevance for providing results that are easy to interpret. For large signal widths, the effect of the detector resolution on the global width is smaller and the difference between the results of the two limit-setting approaches is reduced.

For all signals described above, the following systematic uncertainties are included in the limit setting: jet energy scale, acceptance uncertainties associated to the choice of PDF, and luminosity. The jet energy uncertainty ranges from 1.5% at the lowest masses to 3% for masses above 4.5 TeV. On average, the PDF uncertainty affects the angular distributions by 1%. The uncertainty in the combined 2015 + 2016 integrated luminosity is 3.2%. It is derived, following a methodology similar to that detailed in Ref. [89], from a preliminary calibration of the luminosity scale using x - y beam-separation scans performed in August 2015 and May 2016.

The dijet angular distributions can also be modified by new mediating particles with a mass much higher than that which can be probed directly. A four-fermion effective field theory (contact interaction) characterized by a single energy scale Λ can be used to describe these effects:

$$\begin{aligned} \mathcal{L}_{qq} = \frac{2\pi}{\Lambda^2} & [\eta_{LL} (\bar{q}_L \gamma^\mu q_L) (\bar{q}_L \gamma_\mu q_L) + \eta_{RR} (\bar{q}_R \gamma^\mu q_R) (\bar{q}_R \gamma_\mu q_R) \\ & + 2\eta_{RL} (\bar{q}_R \gamma^\mu q_R) (\bar{q}_L \gamma_\mu q_L)], \end{aligned} \quad (2)$$

where the quark fields have left-handed (L) and right-handed (R) chiral projections and the coefficients η_{LL} , η_{RR} , and η_{RL} activate various interactions. Contact interactions with a nonzero left-chiral color-singlet coupling ($\eta_{LL} = \pm 1$, $\eta_{RL} = \eta_{RR} = 0$) are simulated using PYTHIA

⁵Differences of about 4% between these limits are seen, due to non-Gaussian tails of the resolution which are taken into account by the folding matrix, but are not accounted for in the case of the Gaussian signal at reconstruction level.

TABLE I. Summary of the analysis selection criteria for the three considered signal regions.

	p_T^{leading}	$p_T^{\text{subleading}}$	$ y^* $	$ y_B $	m_{jj}
Resonance	>0.44 TeV	>0.06 TeV	<0.6	\dots	>1.1 TeV
W^*	>0.44 TeV	>0.06 TeV	<1.2	\dots	>1.7 TeV
Angular	>0.44 TeV	>0.06 TeV	<1.7	<1.1	>2.5 TeV

8.816. This type of coupling is chosen because its angular distributions are representative of those of other BSM models (e.g. Z' and others studied here by the resonance search). Interference of the signal model with the SM process $q\bar{q} \rightarrow q\bar{q}$ is included. Events are simulated for both constructive and destructive interference with $\Lambda = 7$ TeV. From this sample, the angular distributions for other values of Λ are obtained using the fact that the interference term is proportional to $1/\Lambda^2$ and the pure contact-interaction cross section is proportional to $1/\Lambda^4$. The PYTHIA signal prediction is reweighted to the NLO cross sections provided by CIJET [90]. Uncertainties in the prediction of the angular

distributions for contact interaction signals are obtained in the same manner as for QCD processes, including JES and PDF uncertainties (as discussed in Sec. VI).

VIII. RESULTS

Starting from the m_{jj} distribution obtained with the resonance search selection, a Bayesian method [16] is applied to the data and simulation of signals at a series of discrete masses to set 95% credibility-level (C.L.) upper limits on the cross section times acceptance for the signals described above. The method uses a constant prior for the signal cross section and Gaussian priors for nuisance parameters corresponding to systematic uncertainties in the signal and background distributions. The expected limits are calculated using pseudoexperiments generated from the maximum-likelihood values of the background uncertainties in the sliding-window background model and accounting for the full set of systematic uncertainties in both the signal and background models. The limit is interpolated logarithmically between the discrete masses

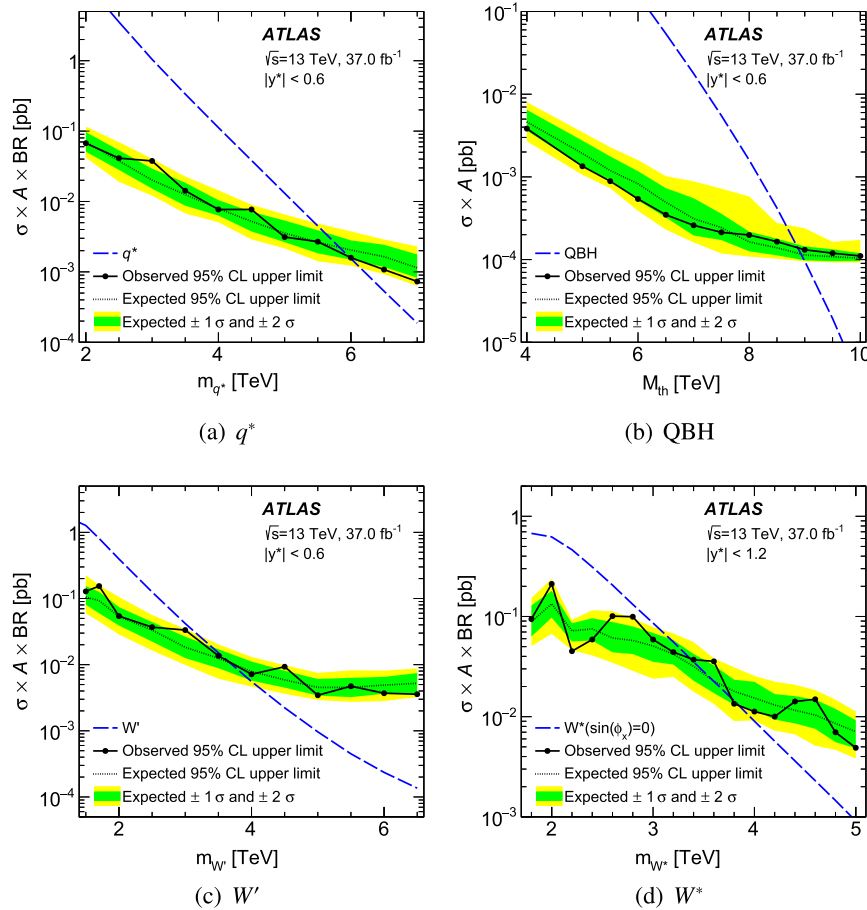


FIG. 3. The 95% C.L. upper limits obtained from the dijet invariant mass (m_{jj}) distribution on cross section times acceptance times branching ratio to two jets, $\sigma \times A \times BR$, for the models described in the text. Clockwise from top left: q^* , quantum black holes with $n = 6$ generated with BLACKMAX, W' , and W^* where the first three use the nominal selection and the last uses the widened $|y^*| < 1.2$ selection. The numerical values of the observed and expected limits are summarized in Table II.

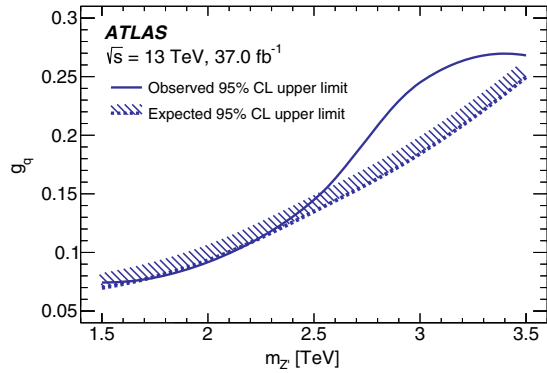


FIG. 4. The 95% C.L. exclusion limits for the Z' model described in the text, as a function of the coupling to quarks, g_q , and the mass, $m_{Z'}$, obtained from the dijet invariant mass m_{jj} distribution. For a given mass, the cross sections rise with g_q , and thus the upper left unfilled area is excluded, as indicated by the direction of the hatched band. The exclusion applies up to $g_q = 0.5$, in the sensitivity range of the method as explained in the text. Points were simulated with 0.5 TeV spacing in mass and spacing as fine as 0.05 in g_q . A smooth curve is drawn between points by interpolating in g_q^2 followed by an interpolation in $m_{Z'}$.

to create continuous exclusion curves. No uncertainty in the theoretical cross section for the signals is assessed. The various selection criteria for the different signal regions are summarized in Table I. The mass limits for each of the models are shown in Figs. 3 and 4 and Table II.

Figure 5 shows limits on the Gaussian contributions to the particle-level m_{jj} distribution obtained for a mean mass m_G and five different widths, from a narrow width to a width of 15% of m_G . The expected limit and the corresponding $\pm 1\sigma$ and $\pm 2\sigma$ bands are also indicated for a narrow-width resonance. Limits are set only when m_G is

TABLE II. The 95% C.L. lower limits on the masses of ADD quantum black holes (BLACKMAX event generator), W' and W^* bosons, excited quarks, and Z' bosons for selected coupling values from the resonance search, as well as on the scale of contact interactions for constructive ($\eta_{LL} = -1$) and destructive ($\eta_{LL} = +1$) interference from the angular analysis. Where an additional range is listed, masses within the range are also excluded. Full limits on the Z' model are provided in Fig. 4.

Model	95% C.L. exclusion limit	
	Observed	Expected
Quantum black hole	8.9 TeV	8.9 TeV
W'	3.6 TeV	3.7 TeV
W^*	3.4 TeV 3.77 TeV—3.85 TeV	3.6 TeV
Excited quark	6.0 TeV	5.8 TeV
Z' ($g_q = 0.1$)	2.1 TeV	2.1 TeV
Z' ($g_q = 0.2$)	2.9 TeV	3.3 TeV
Contact interaction ($\eta_{LL} = -1$)	21.8 TeV	28.3 TeV.
Contact interaction ($\eta_{LL} = +1$)	13.1 TeV 17.4 TeV—29.5 TeV	15.0 TeV

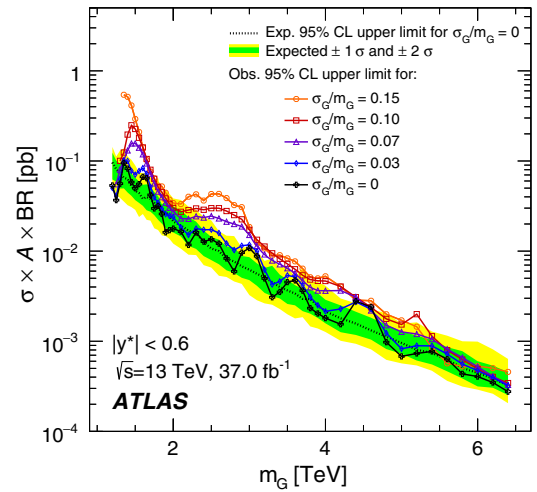


FIG. 5. The 95% C.L. upper limits obtained from the dijet invariant mass m_{jj} distribution on cross section times acceptance times branching ratio to two jets, $\sigma \times A \times BR$, for a hypothetical signal with a cross section σ_G that produces a Gaussian contribution to the particle-level m_{jj} distribution, as a function of the mean of the Gaussian mass distribution m_G . Observed limits are obtained for five different widths, from a narrow width to 15% of m_G . The expected limit and the corresponding $\pm 1\sigma$ and $\pm 2\sigma$ bands are also indicated for a narrow-width resonance.

within 1.1–6.5 TeV and separated by at least the width of the Gaussian resonance from the beginning of this range. Resonances with effective cross sections exceeding values ranging from approximately 20–50 fb for masses of 2 TeV to 0.2–0.5 fb for masses above 6 TeV are excluded. As the width increases, the expected signal contribution is distributed across more bins. Therefore, wider signals are less affected by statistical fluctuations of the data in a single bin than narrower signals.

Starting from the χ distributions obtained with the angular selection, the CL_s method is used to set limits on potential contributions from contact interactions, using the background predicted by the SM simulation as the null hypothesis. The asymptotic approximation [91] of a profile likelihood ratio is used to set 95% C.L. limits. For each value of Λ and each η_{LL} tested, a combined fit is performed on the seven m_{jj} regions of Fig. 2, using the procedure described in Sec. VI. The maximum-likelihood values of the nuisance parameters do not differ significantly from the expectations. The bounds on contact interactions thus obtained are shown in Fig. 6 and in Table II. In the case of destructive interference, the expected event yield including the signal may be lower than that for the background-alone prediction. The kinematic regions where this occurs depend on both Λ and m_{jj} . An observed excess in the data then produces a weaker limit below a given Λ value, and a stronger one above that Λ value, in combination with information from the m_{jj} spectrum in the fit.

The same approach is used to set limits on the resonant benchmark signals described in Sec. VII, as a consistency

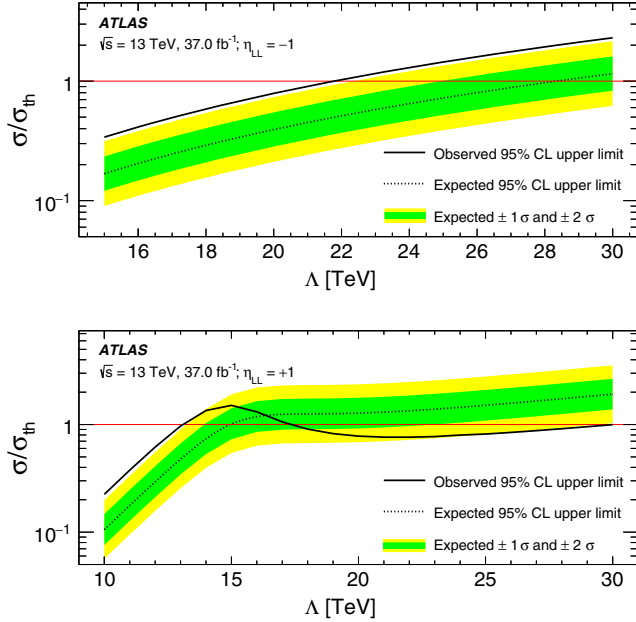


FIG. 6. Ratio $\sigma/\sigma_{\text{th}}$ of the observed and expected 95% C.L. upper limits on the cross section in the contact interaction model to the predicted cross section as a function of the compositeness scale Λ , for constructive (top) and destructive (bottom) interference with QCD processes. The Λ regions for which the observed and expected 95% C.L. lines are below the line at 1.0 represent the observed and expected exclusion regions, respectively. The numerical values of the observed and expected limits are summarized in Table II.

check of the resonance search. The angular analysis has a $\sim 10\%$ lower sensitivity in terms of resonance mass exclusion with respect to the search described in Sec. V.

IX. CONCLUSION

A search for new phenomena beyond the Standard Model has been performed using dijet events in 37.0 fb^{-1} of proton-proton collisions with a center-of-mass energy of $\sqrt{s} = 13 \text{ TeV}$ recorded by the ATLAS detector at the Large Hadron Collider. The dijet invariant mass distribution exhibits no significant local excesses above a data-derived estimate of the smoothly falling distribution predicted by the Standard Model. The two resonant signal regions agree with the background-only hypothesis, with p -values of 0.63 and 0.83 for the $|y^*| < 0.6$ and $|y^*| < 1.2$ selections respectively. The dijet angular distributions, based on the rapidity difference between the two leading jets, also agree with a MC simulation of the SM, with a p -value for the SM-only hypothesis of 0.06. With the resonance selection, the analysis excludes several types of signals at 95% C.L., as predicted by models of quantum black holes, excited quarks, and W' , W^* and Z' bosons. It also sets 95% C.L. upper limits on the cross section for new processes that would produce a Gaussian contribution to the dijet mass distribution. With the angular analysis,

95% C.L. lower limits are set on the compositeness scale of contact interactions for scenarios with either constructive or destructive interference between the new interaction and QCD processes. These results substantially extend the excluded ranges obtained using the 2015 data set alone, with improvements ranging from 7% for quantum black hole masses to 25% for contact interaction scales to 40% for W' boson masses.

ACKNOWLEDGMENTS

We thank CERN for the very successful operation of the LHC, as well as the support staff from our institutions without whom ATLAS could not be operated efficiently. We acknowledge the support of ANPCyT, Argentina; YerPhi, Armenia; ARC, Australia; BMWFW and FWF, Austria; ANAS, Azerbaijan; SSTC, Belarus; CNPq and FAPESP, Brazil; NSERC, NRC and CFI, Canada; CERN; CONICYT, Chile; CAS, MOST and NSFC, China; COLCIENCIAS, Colombia; MSMT CR, MPO CR and VSC CR, Czech Republic; DNRF and DNSRC, Denmark; IN2P3-CNRS, CEA-DSM/IRFU, France; SRNSF, Georgia; BMBF, HGF, and MPG, Germany; GSRT, Greece; RGC, Hong Kong SAR, China; ISF, I-CORE and Benoziyo Center, Israel; INFN, Italy; MEXT and JSPS, Japan; CNRST, Morocco; NWO, Netherlands; RCN, Norway; MNiSW and NCN, Poland; FCT, Portugal; MNE/IFA, Romania; MES of Russia and NRC KI, Russian Federation; JINR; MESTD, Serbia; MSSR, Slovakia; ARRS and MIZŠ, Slovenia; DST/NRF, South Africa; MINECO, Spain; SRC and Wallenberg Foundation, Sweden; SERI, SNSF and Cantons of Bern and Geneva, Switzerland; MOST, Taiwan; TAEK, Turkey; STFC, United Kingdom; DOE and NSF, USA. In addition, individual groups and members have received support from BCKDF, the Canada Council, CANARIE, CRC, Compute Canada, FQRNT, and the Ontario Innovation Trust, Canada; EPLANET, ERC, ERDF, FP7, Horizon 2020 and Marie Skłodowska-Curie Actions, European Union; Investissements d'Avenir Labex and IDEX, ANR, Région Auvergne and Fondation Partager le Savoir, France; DFG and AvH Foundation, Germany; Herakleitos, Thales and Aristeia programmes co-financed by EU-ESF and the Greek NSRF; BSF, GIF and Minerva, Israel; BRF, Norway; CERCA Programme Generalitat de Catalunya, Generalitat Valenciana, Spain; the Royal Society and Leverhulme Trust, United Kingdom. The crucial computing support from all WLCG partners is acknowledged gratefully, in particular from CERN, the ATLAS Tier-1 facilities at TRIUMF (Canada), NDGF (Denmark, Norway, Sweden), CC-IN2P3 (France), KIT/GridKA (Germany), INFN-CNAF (Italy), NL-T1 (Netherlands), PIC (Spain), ASGC (Taiwan), RAL (UK) and BNL (USA), the Tier-2 facilities worldwide and large non-WLCG resource providers. Major contributors of computing resources are listed in Ref. [92].

- [1] L. Evans and P. Bryant, LHC machine, *J. Instrum.* **3**, S08001 (2008)..
- [2] J.M. Campbell, J.W. Huston, and W.J. Stirling, Hard interactions of quarks and gluons: A primer for LHC physics, *Rep. Prog. Phys.* **70**, 89 (2007).
- [3] R.M. Harris and K. Kousouris, Searches for dijet resonances at hadron colliders, *Int. J. Mod. Phys. A* **26**, 5005 (2011).
- [4] N. Boelaert and T. Åkesson, Dijet angular distributions at $\sqrt{s} = 14$ TeV, *Eur. Phys. J. C* **66**, 343 (2010).
- [5] G. Arnison *et al.* (UA1 Collaboration), Angular distributions and structure functions from two jet events at the CERN SPS p anti-p collider, *Phys. Lett.* **136B**, 294 (1984).
- [6] C. Albajar *et al.* (UA1 Collaboration), Two jet mass distributions at the CERN Proton–Anti-Proton Collider, *Phys. Lett. B* **209**, 127 (1988).
- [7] P. Bagnaia *et al.* (UA2 Collaboration), Measurement of jet production properties at the CERN pp Collider, *Phys. Lett.* **144B**, 283 (1984).
- [8] T. Aaltonen *et al.* (CDF Collaboration), Search for new particles decaying into dijets in proton-antiproton collisions at $\sqrt{s} = 1.96$ TeV, *Phys. Rev. D* **79**, 112002 (2009).
- [9] V.M. Abazov *et al.* (D0 Collaboration), Measurement of Dijet Angular Distributions at $\sqrt{s} = 1.96$ TeV and Searches for Quark Compositeness and Extra Spatial Dimensions, *Phys. Rev. Lett.* **103**, 191803 (2009).
- [10] ATLAS Collaboration, Search for New Particles in Two-Jet Final States in 7 TeV Proton-Proton Collisions with the ATLAS Detector at the LHC, *Phys. Rev. Lett.* **105**, 161801 (2010).
- [11] ATLAS Collaboration, Search for quark contact interactions in dijet angular distributions in pp collisions at $\sqrt{s} = 7$ TeV measured with the ATLAS detector, *Phys. Lett. B* **694**, 327 (2011).
- [12] CMS Collaboration, Search for Dijet Resonances in 7 TeV pp Collisions at CMS, *Phys. Rev. Lett.* **105**, 211801 (2010).
- [13] CMS Collaboration, Search for Quark Compositeness with the Dijet Centrality Ratio in pp Collisions at $\sqrt{s} = 7$ TeV, *Phys. Rev. Lett.* **105**, 262001 (2010).
- [14] CMS Collaboration, Measurement of Dijet Angular Distributions and Search for Quark Compositeness in pp Collisions at $\sqrt{s} = 7$ TeV, *Phys. Rev. Lett.* **106**, 201804 (2011).
- [15] CMS Collaboration, Search for resonances in the dijet mass spectrum from 7 TeV pp collisions at CMS, *Phys. Lett. B* **704**, 123 (2011).
- [16] ATLAS Collaboration, A search for new physics in dijet mass and angular distributions in pp collisions at $\sqrt{s} = 7$ TeV measured with the ATLAS detector, *New J. Phys.* **13**, 053044 (2011).
- [17] ATLAS Collaboration, Search for new physics in the dijet mass distribution using 1 fb^{-1} of pp collision data at $\sqrt{s} = 7$ TeV collected by the ATLAS detector, *Phys. Lett. B* **708**, 37 (2012).
- [18] ATLAS Collaboration, ATLAS search for new phenomena in dijet mass and angular distributions using pp collisions at $\sqrt{s} = 7$ TeV, *J. High Energy Phys.* **01** (2013) 029.
- [19] ATLAS Collaboration, Search for new phenomena in the dijet mass distribution using pp collision data at $\sqrt{s} = 8$ TeV with the ATLAS detector, *Phys. Rev. D* **91**, 052007 (2015).
- [20] CMS Collaboration, Search for narrow resonances using the dijet mass spectrum in pp collisions at $\sqrt{s} = 8$ TeV, *Phys. Rev. D* **87**, 114015 (2013).
- [21] ATLAS Collaboration, Search for New Phenomena in Dijet Angular Distributions in Proton–Proton Collisions at $\sqrt{s} = 8$ TeV Measured with the ATLAS Detector, *Phys. Rev. Lett.* **114**, 221802 (2015).
- [22] CMS Collaboration, Search for Narrow Resonances Decaying to Dijets in Proton-Proton Collisions at $\sqrt{s} = 13$ TeV, *Phys. Rev. Lett.* **116**, 071801 (2016).
- [23] ATLAS Collaboration, Search for new phenomena in dijet mass and angular distributions from pp collisions at $\sqrt{s} = 13$ TeV with the ATLAS detector, *Phys. Lett. B* **754**, 302 (2016).
- [24] CMS Collaboration, Search for dijet resonances in proton-proton collisions at $\sqrt{s} = 13$ TeV and constraints on dark matter and other models, *Phys. Lett. B* **769**, 520 (2017).
- [25] ATLAS Collaboration, Search for resonances in the mass distribution of jet pairs with one or two jets identified as b -jets in proton-proton collisions at $\sqrt{s} = 13$ TeV with the ATLAS detector, *Phys. Lett. B* **759**, 229 (2016).
- [26] CMS Collaboration, Search for Narrow Resonances in Dijet Final States at $\sqrt{s} = 8$ TeV with the Novel CMS Technique of Data Scouting, *Phys. Rev. Lett.* **117**, 031802 (2016).
- [27] ATLAS Collaboration, The ATLAS experiment at the CERN Large Hadron Collider, *J. Instrum.* **3**, S08003 (2008).
- [28] ATLAS Collaboration, Report No. ATLAS-TDR-19, 2010, <https://cds.cern.ch/record/1291633>; Report No. ATLAS-TDR-19-ADD-1, 2012, <https://cds.cern.ch/record/1451888>.
- [29] ATLAS Collaboration, Performance of the ATLAS Trigger System in 2015, *Eur. Phys. J. C* **77**, 317 (2017).
- [30] W. Lampl *et al.*, CERN Report No. ATL-LARG-PUB-2008-002, 2008, <https://cds.cern.ch/record/1099735>.
- [31] ATLAS Collaboration, Topological cell clustering in the ATLAS calorimeters and its performance in LHC Run 1, *Eur. Phys. J. C* **77**, 490 (2017).
- [32] M. Cacciari, G. Salam, and G. Soyez, The anti- k_T jet clustering algorithm, *J. High Energy Phys.* **04** (2008) 063.
- [33] M. Cacciari and G. P. Salam, Dispelling the N^3 myth for the k_t jet-finder, *Phys. Lett. B* **641**, 57 (2006).
- [34] ATLAS Collaboration, Report No. ATL-PHYS-PUB-2015-013, <https://cds.cern.ch/record/2022743/>.
- [35] ATLAS Collaboration, Jet energy measurement with the ATLAS detector in proton-proton collisions at $\sqrt{s} = 7$ TeV, *Eur. Phys. J. C* **73**, 2304 (2013).
- [36] ATLAS Collaboration, Jet energy measurement and its systematic uncertainty in proton-proton collisions at $\sqrt{s} = 7$ TeV with the ATLAS detector, *Eur. Phys. J. C* **75**, 17 (2015).
- [37] ATLAS Collaboration, Performance of pile-up mitigation techniques for jets in pp collisions at $\sqrt{s} = 8$ TeV using the ATLAS detector, *Eur. Phys. J. C* **76**, 581 (2016).
- [38] ATLAS Collaboration, Report No. ATLAS-CONF-2015-002, 2015, <https://cds.cern.ch/record/2001682>.
- [39] ATLAS Collaboration, Report No. ATL-PHYS-PUB-2015-015, 2015, <https://cds.cern.ch/record/2037613>.
- [40] ATLAS Collaboration, Jet energy scale measurements and their systematic uncertainties in proton-proton collisions at $\sqrt{s} = 13$ TeV with the ATLAS detector, [arXiv:1703.09665](https://arxiv.org/abs/1703.09665).

- [41] ATLAS Collaboration, Report No. ATLAS-CONF-2015-017, 2015, <https://cds.cern.ch/record/2008678>.
- [42] ATLAS Collaboration, Report No. ATLAS-CONF-2015-057, 2015, <https://cds.cern.ch/record/2059846>.
- [43] ATLAS Collaboration, A measurement of the calorimeter response to single hadrons and determination of the jet energy scale uncertainty using LHC Run-1 pp -collision data with the ATLAS detector, *Eur. Phys. J. C* **77**, 26 (2017).
- [44] ATLAS Collaboration, Report No. ATLAS-CONF-2015-029, 2015, <https://cds.cern.ch/record/2037702>.
- [45] T. Sjöstrand, S. Mrenna, and P. Skands, A brief introduction to Pythia 8.1, *Comput. Phys. Commun.* **178**, 852 (2008).
- [46] ATLAS Collaboration, Report No. ATL-PHYS-PUB-2014-021, 2014, <https://cds.cern.ch/record/1966419>.
- [47] R. D. Ball *et al.*, Parton distributions with LHC data, *Nucl. Phys.* **B867**, 244 (2013).
- [48] S. Agostinelli *et al.*, GEANT4: A simulation toolkit, *Nucl. Instrum. Methods Phys. Res., Sect. A* **506**, 250 (2003).
- [49] ATLAS Collaboration, The ATLAS simulation infrastructure, *Eur. Phys. J. C* **70**, 823 (2010).
- [50] Z. Nagy, Three-Jet Cross Sections in Hadron-Hadron Collisions at Next-to-Leading Order, *Phys. Rev. Lett.* **88**, 122003 (2002).
- [51] Z. Nagy, Next-to-leading order calculation of three-jet observables in hadron-hadron collision, *Phys. Rev. D* **68**, 094002 (2003).
- [52] S. Catani and M. H. Seymour, A general algorithm for calculating jet cross sections in NLO QCD, *Nucl. Phys.* **B485**, 291 (1997).
- [53] S. Dittmaier, A. Huss, and C. Speckner, Weak radiative corrections to dijet production at hadron colliders, *J. High Energy Phys.* **11** (2012) 095.
- [54] U. Baur, I. Hinchliffe, and D. Zeppenfeld, Excited quark production at hadron colliders, *Int. J. Mod. Phys. A* **02**, 1285 (1987).
- [55] U. Baur, M. Spira, and P. M. Zerwas, Excited quark and lepton production at hadron colliders, *Phys. Rev. D* **42**, 815 (1990).
- [56] G. Altarelli, B. Mele, and M. Ruiz-Altaba, Searching for new heavy vector bosons in $p\bar{p}$ colliders, *Z. Phys. C* **45**, 109 (1989); Erratum, *Z. Phys. C* **47**, 676(E) (1990).
- [57] D. Abercrombie *et al.*, Dark matter benchmark models for early LHC Run-2 searches: Report of the ATLAS/CMS Dark Matter Forum, [arXiv:1507.00966](https://arxiv.org/abs/1507.00966).
- [58] M. Chala, F. Kahlhoefer, M. McCullough, G. Nardini, and K. Schmidt-Hoberg, Constraining dark sectors with mono-jets and dijets, *J. High Energy Phys.* **07** (2015) 089.
- [59] M. V. Chizhov, V. A. Bednyakov, and J. A. Budagov, A unique signal of excited bosons in dijet data from pp -collisions, *Phys. At. Nucl.* **75**, 90 (2012).
- [60] M. V. Chizhov and G. Dvali, Origin and phenomenology of weak-doublet spin-1 bosons, *Phys. Lett. B* **703**, 593 (2011).
- [61] D. M. Gingrich, Quantum black holes with charge, colour, and spin at the LHC, *J. Phys. G* **37**, 105008 (2010).
- [62] X. Calmet, W. Gong, and S. D. H. Hsu, Colorful quantum black holes at the LHC, *Phys. Lett. B* **668**, 20 (2008).
- [63] D.-C. Dai, G. Starkman, D. Stojkovic, C. Issever, E. Rizvi, and J. Tseng, BlackMax: A black-hole event generator with rotation, recoil, split branes, and brane tension, *Phys. Rev. D* **77**, 076007 (2008).
- [64] E. Eichten, I. Hinchliffe, K. Lane, and C. Quigg, Super-collider physics, *Rev. Mod. Phys.* **56**, 579 (1984).
- [65] P. Chiapetta and M. Perrottet, Possible bounds on compositeness from inclusive one jet production in large hadron colliders, *Phys. Lett. B* **253**, 489 (1991).
- [66] ATLAS Collaboration, Report No. ATL-SOFT-PUB-2014-01, 2014, <https://cds.cern.ch/record/1669341>.
- [67] T. Aaltonen *et al.* (CDF Collaboration), Global search for new physics with 2.0 fb^{-1} at CDF, *Phys. Rev. D* **79**, 011101 (2009).
- [68] G. Choudalakis, On hypothesis testing, trials factor, hypertests and the BumpHunter, [arXiv:1101.0390](https://arxiv.org/abs/1101.0390).
- [69] N. Boelaert, *Dijet Angular Distributions in Proton-Proton Collisions* (Springer-Verlag Berlin Heidelberg, 2012), <http://www.springer.com/us/book/9783642245961>.
- [70] H.-L. Lai, M. Guzzi, J. Huston, Z. Li, P. M. Nadolsky, J. Pumplin, and C.-P. Yuan, New parton distributions for collider physics, *Phys. Rev. D* **82**, 074024 (2010).
- [71] A. D. Martin, W. J. Stirling, R. S. Thorne, and G. Watt, Parton distributions for the LHC, *Eur. Phys. J. C* **63**, 189 (2009).
- [72] A. L. Read, Presentation of search results: The CL(s) technique, *J. Phys. G* **28**, 2693 (2002).
- [73] T. Junk, Confidence level computation for combining searches with small statistics, *Nucl. Instrum. Methods Phys. Res., Sect. A* **434**, 435 (1999).
- [74] S. B. Giddings and S. D. Thomas, High-energy colliders as black hole factories: the end of short distance physics, *Phys. Rev. D* **65**, 056010 (2002).
- [75] S. Dimopoulos and G. L. Landsberg, Black Holes at the Large Hadron Collider, *Phys. Rev. Lett.* **87**, 161602 (2001).
- [76] P. Meade and L. Randall, Black holes and quantum gravity at the LHC, *J. High Energy Phys.* **05** (2008) 003.
- [77] L. A. Anchordoqui, J. L. Feng, H. Goldberg, and A. D. Shapere, Inelastic black hole production and large extra dimensions, *Phys. Lett. B* **594**, 363 (2004).
- [78] ATLAS Collaboration, Search for strong gravity in multijet final states produced in pp collisions at $\sqrt{s} = 13 \text{ TeV}$ using the ATLAS detector at the LHC, *J. High Energy Phys.* **03** (2016) 026.
- [79] ATLAS Collaboration, Search for TeV-scale gravity signatures in high-mass final states with leptons and jets with the ATLAS detector at $\sqrt{s} = 13 \text{ TeV}$, *Phys. Lett. B* **760**, 520 (2016).
- [80] CMS Collaboration, Search for microscopic black holes in pp collisions at $\sqrt{s} = 8 \text{ TeV}$, *J. High Energy Phys.* **07** (2013) 178.
- [81] J. A. Frost, J. R. Gaunt, M. O. P. Sampaio, M. Casals, S. R. Dolan, M. A. Parker, and B. R. Webber, Phenomenology of production and decay of spinning extra-dimensional black holes at hadron colliders, *J. High Energy Phys.* **10** (2009) 014.
- [82] N. Arkani-Hamed, S. Dimopoulos, and G. R. Dvali, The hierarchy problem and new dimensions at a millimeter, *Phys. Lett. B* **429**, 263 (1998).
- [83] I. Antoniadis, N. Arkani-Hamed, S. Dimopoulos, and G. R. Dvali, New dimensions at a millimeter to a Fermi and superstrings at a TeV, *Phys. Lett. B* **436**, 257 (1998).
- [84] J. Pumplin, D. R. Stump, J. Huston, H.-L. Lai, P. Nadolsky, and W.-K. Tung, New generation of parton distributions

- with uncertainties from global QCD analysis, *J. High Energy Phys.* **07** (2002) 012.
- [85] P. Langacker, R. W. Robinett, and J. L. Rosner, New heavy gauge bosons in pp and $p\bar{p}$ collisions, *Phys. Rev. D* **30**, 1470 (1984).
- [86] J. Alwall, R. Frederix, S. Frixione, V. Hirschi, F. Maltoni, O. Mattelaer, H.-S. Shao, T. Stelzer, P. Torrielli, and M. Zaro, The automated computation of tree-level and next-to-leading order differential cross sections, and their matching to parton shower simulations, *J. High Energy Phys.* **07** (2014) 079.
- [87] M. V. Chizhov, A reference model for anomalously interacting bosons, *Phys. Part. Nucl. Lett.* **8**, 512 (2011).
- [88] A. Belyaev, N. D. Christensen, and A. Pukhov, CalcHEP 3.4 for collider physics within and beyond the standard model, *Comput. Phys. Commun.* **184**, 1729 (2013).
- [89] ATLAS Collaboration, Luminosity determination in pp collisions at $\sqrt{s} = 8$ TeV using the ATLAS detector at the LHC, *Eur. Phys. J. C* **76**, 653 (2016).
- [90] J. Gao, CIJET: A program for computation of jet cross sections induced by quark contact interactions at hadron colliders, *Comput. Phys. Commun.* **184**, 2362 (2013).
- [91] G. Cowan, K. Cranmer, E. Gross, and O. Vitells, Asymptotic formulae for likelihood-based tests of new physics, *Eur. Phys. J. C* **71**, 1554 (2011).
- [92] ATLAS Collaboration, Report No. ATL-GEN-PUB-2016-002, 2016, <https://cds.cern.ch/record/2202407>.

M. Aaboud,^{137d} G. Aad,⁸⁸ B. Abbott,¹¹⁵ J. Abdallah,⁸ O. Abdinov,^{12,a} B. Abeloos,¹¹⁹ S. H. Abidi,¹⁶¹ O. S. AbouZeid,¹³⁹ N. L. Abraham,¹⁵¹ H. Abramowicz,¹⁵⁵ H. Abreu,¹⁵⁴ R. Abreu,¹¹⁸ Y. Abulaiti,^{148a,148b} B. S. Acharya,^{167a,167b,b} S. Adachi,¹⁵⁷ L. Adamczyk,^{41a} J. Adelman,¹¹⁰ M. Adersberger,¹⁰² T. Adye,¹³³ A. A. Affolder,¹³⁹ T. Agatonovic-Jovin,¹⁴ C. Agheorghiesei,^{28c} J. A. Aguilar-Saavedra,^{128a,128f} S. P. Ahlen,²⁴ F. Ahmadov,^{68,c} G. Aielli,^{135a,135b} S. Akatsuka,⁷¹ H. Akerstedt,^{148a,148b} T. P. A. Åkesson,⁸⁴ A. V. Akimov,⁹⁸ G. L. Alberghi,^{22a,22b} J. Albert,¹⁷² P. Albicocco,⁵⁰ M. J. Alconada Verzini,⁷⁴ M. Aleksa,³² I. N. Aleksandrov,⁶⁸ C. Alexa,^{28b} G. Alexander,¹⁵⁵ T. Alexopoulos,¹⁰ M. Alhroob,¹¹⁵ B. Ali,¹³⁰ M. Aliev,^{76a,76b} G. Alimonti,^{94a} J. Alison,³³ S. P. Alkire,³⁸ B. M. M. Allbrooke,¹⁵¹ B. W. Allen,¹¹⁸ P. P. Allport,¹⁹ A. Aloisio,^{106a,106b} A. Alonso,³⁹ F. Alonso,⁷⁴ C. Alpigiani,¹⁴⁰ A. A. Alshehri,⁵⁶ M. Alstaty,⁸⁸ B. Alvarez Gonzalez,³² D. Álvarez Piqueras,¹⁷⁰ M. G. Alviggi,^{106a,106b} B. T. Amadio,¹⁶ Y. Amaral Coutinho,^{26a} C. Amelung,²⁵ D. Amidei,⁹² S. P. Amor Dos Santos,^{128a,128c} A. Amorim,^{128a,128b} S. Amoroso,³² G. Amundsen,²⁵ C. Anastopoulos,¹⁴¹ L. S. Ancu,⁵² N. Andari,¹⁹ T. Andeen,¹¹ C. F. Anders,^{60b} J. K. Anders,⁷⁷ K. J. Anderson,³³ A. Andreazza,^{94a,94b} V. Andrei,^{60a} S. Angelidakis,⁹ I. Angelozzi,¹⁰⁹ A. Angerami,³⁸ A. V. Anisenkov,^{111,d} N. Anjos,¹³ A. Annovi,^{126a,126b} C. Antel,^{60a} M. Antonelli,⁵⁰ A. Antonov,^{100,a} D. J. Antrim,¹⁶⁶ F. Anulli,^{134a} M. Aoki,⁶⁹ L. Aperio Bella,³² G. Arabidze,⁹³ Y. Arai,⁶⁹ J. P. Araque,^{128a} V. Araujo Ferraz,^{26a} A. T. H. Arce,⁴⁸ R. E. Ardell,⁸⁰ F. A. Arduh,⁷⁴ J.-F. Arguin,⁹⁷ S. Argyropoulos,⁶⁶ M. Arik,^{20a} A. J. Armbruster,¹⁴⁵ L. J. Armitage,⁷⁹ O. Arnaez,¹⁶¹ H. Arnold,⁵¹ M. Arratia,³⁰ O. Arslan,²³ A. Artamonov,⁹⁹ G. Artoni,¹²² S. Artz,⁸⁶ S. Asai,¹⁵⁷ N. Asbah,⁴⁵ A. Ashkenazi,¹⁵⁵ L. Asquith,¹⁵¹ K. Assamagan,²⁷ R. Astalos,^{146a} M. Atkinson,¹⁶⁹ N. B. Atlay,¹⁴³ K. Augsten,¹³⁰ G. Avolio,³² B. Axen,¹⁶ M. K. Ayoub,¹¹⁹ G. Azuelos,^{97,e} A. E. Baas,^{60a} M. J. Baca,¹⁹ H. Bachacou,¹³⁸ K. Bachas,^{76a,76b} M. Backes,¹²² M. Backhaus,³² P. Bagnaia,^{134a,134b} H. Bahrasemani,¹⁴⁴ J. T. Baines,¹³³ M. Bajic,³⁹ O. K. Baker,¹⁷⁹ E. M. Baldin,^{111,d} P. Balek,¹⁷⁵ F. Balli,¹³⁸ W. K. Balunas,¹²⁴ E. Banas,⁴² Sw. Banerjee,^{176,f} A. A. E. Bannoura,¹⁷⁸ L. Barak,³² E. L. Barberio,⁹¹ D. Barberis,^{53a,53b} M. Barbero,⁸⁸ T. Barillari,¹⁰³ M.-S. Barisits,³² T. Barklow,¹⁴⁵ N. Barlow,³⁰ S. L. Barnes,^{36c} B. M. Barnett,¹³³ R. M. Barnett,¹⁶ Z. Barnovska-Blenessy,^{36a} A. Baroncelli,^{136a} G. Barone,²⁵ A. J. Barr,¹²² L. Barranco Navarro,¹⁷⁰ F. Barreiro,⁸⁵ J. Barreiro Guimarães da Costa,^{35a} R. Bartoldus,¹⁴⁵ A. E. Barton,⁷⁵ P. Bartos,^{146a} A. Basalaeu,¹²⁵ A. Bassalat,^{119,g} R. L. Bates,⁵⁶ S. J. Batista,¹⁶¹ J. R. Batley,³⁰ M. Battaglia,¹³⁹ M. Bauce,^{134a,134b} F. Bauer,¹³⁸ H. S. Bawa,^{145,h} J. B. Beacham,¹¹³ M. D. Beattie,⁷⁵ T. Beau,⁸³ P. H. Beauchemin,¹⁶⁵ P. Bechtel,²³ H. P. Beck,^{18,i} K. Becker,¹²² M. Becker,⁸⁶ M. Beckingham,¹⁷³ C. Becot,¹¹² A. J. Beddall,^{20e} A. Beddall,^{20b} V. A. Bednyakov,⁶⁸ M. Bedognetti,¹⁰⁹ C. P. Bee,¹⁵⁰ T. A. Beermann,³² M. Begalli,^{26a} M. Begel,²⁷ J. K. Behr,⁴⁵ A. S. Bell,⁸¹ G. Bella,¹⁵⁵ L. Bellagamba,^{22a} A. Bellerive,³¹ M. Bellomo,¹⁵⁴ K. Belotskiy,¹⁰⁰ O. Beltramello,³² N. L. Belyaev,¹⁰⁰ O. Benary,^{155,a} D. Benckekroun,^{137a} M. Bender,¹⁰² K. Bendtz,^{148a,148b} N. Benekos,¹⁰ Y. Benhammou,¹⁵⁵ E. Benhar Noccioli,¹⁷⁹ J. Benitez,⁶⁶ D. P. Benjamin,⁴⁸ M. Benoit,⁵² J. R. Bensinger,²⁵ S. Bentvelsen,¹⁰⁹ L. Beresford,¹²² M. Beretta,⁵⁰ D. Berge,¹⁰⁹ E. Bergeaas Kuutmann,¹⁶⁸ N. Berger,⁵ J. Beringer,¹⁶ S. Berlendis,⁵⁸ N. R. Bernard,⁸⁹ G. Bernardi,⁸³ C. Bernius,¹⁴⁵ F. U. Bernlochner,²³ T. Berry,⁸⁰ P. Berta,¹³¹ C. Bertella,^{35a} G. Bertoli,^{148a,148b} F. Bertolucci,^{126a,126b} I. A. Bertram,⁷⁵ C. Bertsche,⁴⁵ D. Bertsche,¹¹⁵ G. J. Besjes,³⁹ O. Bessidskaia Bylund,^{148a,148b} M. Bessner,⁴⁵ N. Besson,¹³⁸ C. Betancourt,⁵¹ A. Bethani,⁸⁷ S. Bethke,¹⁰³ A. J. Bevan,⁷⁹ J. Beyer,¹⁰³ R. M. Bianchi,¹²⁷ O. Biebel,¹⁰² D. Biedermann,¹⁷ R. Bielski,⁸⁷ N. V. Biesuz,^{126a,126b} M. Biglietti,^{136a} J. Bilbao De Mendizabal,⁵²

T. R. V. Billoud,⁹⁷ H. Bilokon,⁵⁰ M. Bindi,⁵⁷ A. Bingul,^{20b} C. Bini,^{134a,134b} S. Biondi,^{22a,22b} T. Bisanz,⁵⁷ C. Bittrich,⁴⁷ D. M. Bjergaard,⁴⁸ C. W. Black,¹⁵² J. E. Black,¹⁴⁵ K. M. Black,²⁴ R. E. Blair,⁶ T. Blazek,^{146a} I. Bloch,⁴⁵ C. Blocker,²⁵ A. Blue,⁵⁶ W. Blum,^{86,a} U. Blumenschein,⁷⁹ S. Blunier,^{34a} G. J. Bobbink,¹⁰⁹ V. S. Bobrovnikov,^{111,d} S. S. Bocchetta,⁸⁴ A. Bocci,⁴⁸ C. Bock,¹⁰² M. Boehler,⁵¹ D. Boerner,¹⁷⁸ D. Bogavac,¹⁰² A. G. Bogdanchikov,¹¹¹ C. Bohm,^{148a} V. Boisvert,⁸⁰ P. Bokan,^{168,j} T. Bold,^{41a} A. S. Boldyrev,¹⁰¹ A. E. Bolz,^{60b} M. Bomben,⁸³ M. Bona,⁷⁹ M. Boonekamp,¹³⁸ A. Borisov,¹³² G. Borissov,⁷⁵ J. Bortfeldt,³² D. Bortoletto,¹²² V. Bortolotto,^{62a,62b,62c} D. Boscherini,^{22a} M. Bosman,¹³ J. D. Bossio Sola,²⁹ J. Boudreau,¹²⁷ J. Bouffard,² E. V. Bouhova-Thacker,⁷⁵ D. Boumediene,³⁷ C. Bourdarios,¹¹⁹ S. K. Boutle,⁵⁶ A. Boveia,¹¹³ J. Boyd,³² I. R. Boyko,⁶⁸ J. Bracini,¹⁹ A. Brandt,⁸ G. Brandt,⁵⁷ O. Brandt,^{60a} U. Bratzler,¹⁵⁸ B. Brau,⁸⁹ J. E. Brau,¹¹⁸ W. D. Breaden Madden,⁵⁶ K. Brendlinger,⁴⁵ A. J. Brennan,⁹¹ L. Brenner,¹⁰⁹ R. Brenner,¹⁶⁸ S. Bressler,¹⁷⁵ D. L. Briglin,¹⁹ T. M. Bristow,⁴⁹ D. Britton,⁵⁶ D. Britzger,⁴⁵ F. M. Brochu,³⁰ I. Brock,²³ R. Brock,⁹³ G. Brooijmans,³⁸ T. Brooks,⁸⁰ W. K. Brooks,^{34b} J. Brosamer,¹⁶ E. Brost,¹¹⁰ J. H. Broughton,¹⁹ P. A. Bruckman de Renstrom,⁴² D. Bruncko,^{146b} A. Bruni,^{22a} G. Bruni,^{22a} L. S. Bruni,¹⁰⁹ B. H. Brunt,³⁰ M. Bruschi,^{22a} N. Brusino,²³ P. Bryant,³³ L. Bryngemark,⁴⁵ T. Buanes,¹⁵ Q. Buat,¹⁴⁴ P. Buchholz,¹⁴³ A. G. Buckley,⁵⁶ I. A. Budagov,⁶⁸ F. Buehrer,⁵¹ M. K. Bugge,¹²¹ O. Bulekov,¹⁰⁰ D. Bullock,⁸ T. J. Burch,¹¹⁰ H. Burckhart,³² S. Burdin,⁷⁷ C. D. Burgard,⁵¹ A. M. Burger,⁵ B. Burghgrave,¹¹⁰ K. Burka,⁴² S. Burke,¹³³ I. Burmeister,⁴⁶ J. T. P. Burr,¹²² E. Busato,³⁷ D. Büscher,⁵¹ V. Büscher,⁸⁶ P. Bussey,⁵⁶ J. M. Butler,²⁴ C. M. Buttar,⁵⁶ J. M. Butterworth,⁸¹ P. Butti,³² W. Buttinger,²⁷ A. Buzatu,^{35c} A. R. Buzykaev,^{111,d} S. Cabrera Urbán,¹⁷⁰ D. Caforio,¹³⁰ V. M. Cairo,^{40a,40b} O. Cakir,^{4a} N. Calace,⁵² P. Calafiura,¹⁶ A. Calandri,⁸⁸ G. Calderini,⁸³ P. Calfayan,⁶⁴ G. Callea,^{40a,40b} L. P. Caloba,^{26a} S. Calvente Lopez,⁸⁵ D. Calvet,³⁷ S. Calvet,³⁷ T. P. Calvet,⁸⁸ R. Camacho Toro,³³ S. Camarda,³² P. Camarri,^{135a,135b} D. Cameron,¹²¹ R. Caminal Armadans,¹⁶⁹ C. Camincher,⁵⁸ S. Campana,³² M. Campanelli,⁸¹ A. Camplani,^{94a,94b} A. Campoverde,¹⁴³ V. Canale,^{106a,106b} M. Cano Bret,^{36c} J. Cantero,¹¹⁶ T. Cao,¹⁵⁵ M. D. M. Capeans Garrido,³² I. Caprini,^{28b} M. Caprini,^{28b} M. Capua,^{40a,40b} R. M. Carbone,³⁸ R. Cardarelli,^{135a} F. Cardillo,⁵¹ I. Carli,¹³¹ T. Carli,³² G. Carlino,^{106a} B. T. Carlson,¹²⁷ L. Carminati,^{94a,94b} R. M. D. Carney,^{148a,148b} S. Caron,¹⁰⁸ E. Carquin,^{34b} S. Carrá,^{94a,94b} G. D. Carrillo-Montoya,³² J. Carvalho,^{128a,128c} D. Casadei,¹⁹ M. P. Casado,^{13,k} M. Casolino,¹³ D. W. Casper,¹⁶⁶ R. Castelijin,¹⁰⁹ V. Castillo Gimenez,¹⁷⁰ N. F. Castro,^{128a,l} A. Catinaccio,³² J. R. Catmore,¹²¹ A. Cattai,³² J. Caudron,²³ V. Cavaliere,¹⁶⁹ E. Cavallaro,¹³ D. Cavalli,^{94a} M. Cavalli-Sforza,¹³ V. Cavasinni,^{126a,126b} E. Celebi,^{20a} F. Ceradini,^{136a,136b} L. Cerda Alberich,¹⁷⁰ A. S. Cerqueira,^{26b} A. Cerri,¹⁵¹ L. Cerrito,^{135a,135b} F. Cerutti,¹⁶ A. Cervelli,¹⁸ S. A. Cetin,^{20d} A. Chafaq,^{137a} D. Chakraborty,¹¹⁰ S. K. Chan,⁵⁹ W. S. Chan,¹⁰⁹ Y. L. Chan,^{62a} P. Chang,¹⁶⁹ J. D. Chapman,³⁰ D. G. Charlton,¹⁹ C. C. Chau,¹⁶¹ C. A. Chavez Barajas,¹⁵¹ S. Che,¹¹³ S. Cheatham,^{167a,167c} A. Chegwidien,⁹³ S. Chekanov,⁶ S. V. Chekulaev,^{163a} G. A. Chelkov,^{68,m} M. A. Chelstowska,³² C. Chen,⁶⁷ H. Chen,²⁷ S. Chen,^{35b} S. Chen,¹⁵⁷ X. Chen,^{35c,n} Y. Chen,⁷⁰ H. C. Cheng,⁹² H. J. Cheng,^{35a} A. Cheplakov,⁶⁸ E. Cheremushkina,¹³² R. Cherkou El Moursli,^{137e} V. Chernyatin,^{27,a} E. Cheu,⁷ K. Cheung,⁶³ L. Chevalier,¹³⁸ V. Chiarella,⁵⁰ G. Chiarelli,^{126a,126b} G. Chiodini,^{76a} A. S. Chisholm,³² A. Chitan,^{28b} Y. H. Chiu,¹⁷² M. V. Chizhov,⁶⁸ K. Choi,⁶⁴ A. R. Chomont,³⁷ S. Chouridou,¹⁵⁶ V. Christodoulou,⁸¹ D. Chromek-Burckhart,³² M. C. Chu,^{62a} J. Chudoba,¹²⁹ A. J. Chuinard,⁹⁰ J. J. Chwastowski,⁴² L. Chytka,¹¹⁷ A. K. Ciftci,^{4a} D. Cinca,⁴⁶ V. Cindro,⁷⁸ I. A. Cioara,²³ C. Ciocca,^{22a,22b} A. Ciocio,¹⁶ F. Ciotto,^{106a,106b} Z. H. Citron,¹⁷⁵ M. Citterio,^{94a} M. Ciubancan,^{28b} A. Clark,⁵² B. L. Clark,⁵⁹ M. R. Clark,³⁸ P. J. Clark,⁴⁹ R. N. Clarke,¹⁶ C. Clement,^{148a,148b} Y. Coadou,⁸⁸ M. Cobal,^{167a,167c} A. Coccaro,⁵² J. Cochran,⁶⁷ L. Colasurdo,¹⁰⁸ B. Cole,³⁸ A. P. Colijn,¹⁰⁹ J. Collot,⁵⁸ T. Colombo,¹⁶⁶ P. Conde Muiño,^{128a,128b} E. Coniavitis,⁵¹ S. H. Connell,^{147b} I. A. Connelly,⁸⁷ S. Constantinescu,^{28b} G. Conti,³² F. Conventi,^{106a,o} M. Cooke,¹⁶ A. M. Cooper-Sarkar,¹²² F. Cormier,¹⁷¹ K. J. R. Cormier,¹⁶¹ M. Corradi,^{134a,134b} F. Corriveau,^{90,p} A. Cortes-Gonzalez,³² G. Cortiana,¹⁰³ G. Costa,^{94a} M. J. Costa,¹⁷⁰ D. Costanzo,¹⁴¹ G. Cottin,³⁰ G. Cowan,⁸⁰ B. E. Cox,⁸⁷ K. Cranmer,¹¹² S. J. Crawley,⁵⁶ R. A. Creager,¹²⁴ G. Cree,³¹ S. Crépe-Renaudin,⁵⁸ F. Crescioli,⁸³ W. A. Cribbs,^{148a,148b} M. Cristinziani,²³ V. Croft,¹⁰⁸ G. Crosetti,^{40a,40b} A. Cueto,⁸⁵ T. Cuhadar Donszelmann,¹⁴¹ A. R. Cukierman,¹⁴⁵ J. Cummings,¹⁷⁹ M. Curatolo,⁵⁰ J. Cúth,⁸⁶ H. Czirr,¹⁴³ P. Czodrowski,³² G. D'amen,^{22a,22b} S. D'Auria,⁵⁶ L. D'eraimo,⁸³ M. D'Onofrio,⁷⁷ M. J. Da Cunha Sargedas De Sousa,^{128a,128b} C. Da Via,⁸⁷ W. Dabrowski,^{41a} T. Dado,^{146a} T. Dai,⁹² O. Dale,¹⁵ F. Dallaire,⁹⁷ C. Dallapiccola,⁸⁹ M. Dam,³⁹ J. R. Dandoy,¹²⁴ M. F. Daneri,²⁹ N. P. Dang,¹⁷⁶ A. C. Daniells,¹⁹ N. S. Dann,⁸⁷ M. Danninger,¹⁷¹ M. Dano Hoffmann,¹³⁸ V. Dao,¹⁵⁰ G. Darbo,^{53a} S. Darmora,⁸ J. Dassoulas,³ A. Dattagupta,¹¹⁸ T. Daubney,⁴⁵ W. Davey,²³ C. David,⁴⁵ T. Davidek,¹³¹ M. Davies,¹⁵⁵ D. R. Davis,⁴⁸ P. Davison,⁸¹ E. Dawe,⁹¹ I. Dawson,¹⁴¹ K. De,⁸ R. de Asmundis,^{106a} A. De Benedetti,¹¹⁵ S. De Castro,^{22a,22b} S. De Cecco,⁸³ N. De Groot,¹⁰⁸ P. de Jong,¹⁰⁹ H. De la Torre,⁹³ F. De Lorenzi,⁶⁷ A. De Maria,⁵⁷ D. De Pedis,^{134a} A. De Salvo,^{134a} U. De Sanctis,^{135a,135b} A. De Santo,¹⁵¹ K. De Vasconcelos Corga,⁸⁸

J. B. De Vivie De Regie,¹¹⁹ W. J. Dearnaley,⁷⁵ R. Debbe,²⁷ C. Debenedetti,¹³⁹ D. V. Dedovich,⁶⁸ N. Dehghanian,³ I. Deigaard,¹⁰⁹ M. Del Gaudio,^{40a,40b} J. Del Peso,⁸⁵ T. Del Prete,^{126a,126b} D. Delgove,¹¹⁹ F. Deliot,¹³⁸ C. M. Delitzsch,⁵² A. Dell'Acqua,³² L. Dell'Asta,²⁴ M. Dell'Orso,^{126a,126b} M. Della Pietra,^{106a,106b} D. della Volpe,⁵² M. Delmastro,⁵ C. Delporte,¹¹⁹ P. A. Delsart,⁵⁸ D. A. DeMarco,¹⁶¹ S. Demers,¹⁷⁹ M. Demichev,⁶⁸ A. Demilly,⁸³ S. P. Denisov,¹³² D. Denysiuk,¹³⁸ D. Derendarz,⁴² J. E. Derkaoui,^{137d} F. Derue,⁸³ P. Dervan,⁷⁷ K. Desch,²³ C. Deterre,⁴⁵ K. Dette,⁴⁶ M. R. Devesa,²⁹ P. O. Deviveiros,³² A. Dewhurst,¹³³ S. Dhaliwal,²⁵ F. A. Di Bello,⁵² A. Di Ciaccio,^{135a,135b} L. Di Ciaccio,⁵ W. K. Di Clemente,¹²⁴ C. Di Donato,^{106a,106b} A. Di Girolamo,³² B. Di Girolamo,³² B. Di Micco,^{136a,136b} R. Di Nardo,³² K. F. Di Petrillo,⁵⁹ A. Di Simone,⁵¹ R. Di Sipio,¹⁶¹ D. Di Valentino,³¹ C. Diaconu,⁸⁸ M. Diamond,¹⁶¹ F. A. Dias,³⁹ M. A. Diaz,^{34a} E. B. Diehl,⁹² J. Dietrich,¹⁷ S. Díez Cornell,⁴⁵ A. Dimitrievska,¹⁴ J. Dingfelder,²³ P. Dita,^{28b} S. Dita,^{28b} F. Dittus,³² F. Djama,⁸⁸ T. Djobava,^{54b} J. I. Djuvsland,^{60a} M. A. B. do Vale,^{26c} D. Dobos,³² M. Dobre,^{28b} C. Doglioni,⁸⁴ J. Dolejsi,¹³¹ Z. Dolezal,¹³¹ M. Donadelli,^{26d} S. Donati,^{126a,126b} P. Dondero,^{123a,123b} J. Donini,³⁷ J. Dopke,¹³³ A. Doria,^{106a} M. T. Dova,⁷⁴ A. T. Doyle,⁵⁶ E. Drechsler,⁵⁷ M. Dris,¹⁰ Y. Du,^{36b} J. Duarte-Campderros,¹⁵⁵ A. Dubreuil,⁵² E. Duchovni,¹⁷⁵ G. Duckeck,¹⁰² A. Ducourthial,⁸³ O. A. Ducu,^{97q} D. Duda,¹⁰⁹ A. Dudarev,³² A. Chr. Dudder,⁸⁶ E. M. Duffield,¹⁶ L. Dufлот,¹¹⁹ M. Dührssen,³² M. Dumancic,¹⁷⁵ A. E. Dumitriu,^{28b} A. K. Duncan,⁵⁶ M. Dunford,^{60a} H. Duran Yildiz,^{4a} M. Düren,⁵⁵ A. Durglishvili,^{54b} D. Duschinger,⁴⁷ B. Dutta,⁴⁵ M. Dyndal,⁴⁵ C. Eckardt,⁴⁵ K. M. Ecker,¹⁰³ R. C. Edgar,⁹² T. Eifert,³² G. Eigen,¹⁵ K. Einsweiler,¹⁶ T. Ekelof,¹⁶⁸ M. El Kacimi,^{137c} R. El Kosseifi,⁸⁸ V. Ellajosyula,⁸⁸ M. Ellert,¹⁶⁸ S. Elles,⁵ F. Ellinghaus,¹⁷⁸ A. A. Elliot,¹⁷² N. Ellis,³² J. Elmsheuser,²⁷ M. Elsing,³² D. Emelianov,¹³³ Y. Enari,¹⁵⁷ O. C. Endner,⁸⁶ J. S. Ennis,¹⁷³ J. Erdmann,⁴⁶ A. Ereditato,¹⁸ G. Ernis,¹⁷⁸ M. Ernst,²⁷ S. Errede,¹⁶⁹ M. Escalier,¹¹⁹ C. Escobar,¹²⁷ B. Esposito,⁵⁰ O. Estrada Pastor,¹⁷⁰ A. I. Etienvre,¹³⁸ E. Etzion,¹⁵⁵ H. Evans,⁶⁴ A. Ezhilov,¹²⁵ M. Ezzi,^{137e} F. Fabbri,^{22a,22b} L. Fabbri,^{22a,22b} G. Facini,³³ R. M. Fakhruddinov,¹³² S. Falciano,^{134a} R. J. Falla,⁸¹ J. Faltova,³² Y. Fang,^{35a} M. Fanti,^{94a,94b} A. Farbin,⁸ A. Farilla,^{136a} C. Farina,¹²⁷ E. M. Farina,^{123a,123b} T. Farooque,⁹³ S. Farrell,¹⁶ S. M. Farrington,¹⁷³ P. Farthouat,³² F. Fassi,^{137e} P. Fassnacht,³² D. Fassouliotis,⁹ M. Fauci Giannelli,⁸⁰ A. Favareto,^{53a,53b} W. J. Fawcett,¹²² L. Fayard,¹¹⁹ O. L. Fedin,^{125,r} W. Fedorko,¹⁷¹ S. Feigl,¹²¹ L. Feligioni,⁸⁸ C. Feng,^{36b} E. J. Feng,³² H. Feng,⁹² M. J. Fenton,⁵⁶ A. B. Fenyuk,¹³² L. Feremenga,⁸ P. Fernandez Martinez,¹⁷⁰ S. Fernandez Perez,¹³ J. Ferrando,⁴⁵ A. Ferrari,¹⁶⁸ P. Ferrari,¹⁰⁹ R. Ferrari,^{123a} D. E. Ferreira de Lima,^{60b} A. Ferrer,¹⁷⁰ D. Ferrere,⁵² C. Ferretti,⁹² F. Fiedler,⁸⁶ A. Filipčič,⁷⁸ M. Filipuzzi,⁴⁵ F. Filthaut,¹⁰⁸ M. Fincke-Keeler,¹⁷² K. D. Finelli,¹⁵² M. C. N. Fiolhais,^{128a,128c,s} L. Fiorini,¹⁷⁰ A. Fischer,² C. Fischer,¹³ J. Fischer,¹⁷⁸ W. C. Fisher,⁹³ N. Flaschel,⁴⁵ I. Fleck,¹⁴³ P. Fleischmann,⁹² R. R. M. Fletcher,¹²⁴ T. Flick,¹⁷⁸ B. M. Flierl,¹⁰² L. R. Flores Castillo,^{62a} M. J. Flowerdew,¹⁰³ G. T. Forcolin,⁸⁷ A. Formica,¹³⁸ F. A. Förster,¹³ A. Forti,⁸⁷ A. G. Foster,¹⁹ D. Fournier,¹¹⁹ H. Fox,⁷⁵ S. Fracchia,¹⁴¹ P. Francavilla,⁸³ M. Franchini,^{22a,22b} S. Franchino,^{60a} D. Francis,³² L. Franconi,¹²¹ M. Franklin,⁵⁹ M. Frate,¹⁶⁶ M. Fraternali,^{123a,123b} D. Freeborn,⁸¹ S. M. Fressard-Batraneanu,³² B. Freund,⁹⁷ D. Froidevaux,³² J. A. Frost,¹²² C. Fukunaga,¹⁵⁸ T. Fusayasu,¹⁰⁴ J. Fuster,¹⁷⁰ C. Gabaldon,⁵⁸ O. Gabizon,¹⁵⁴ A. Gabrielli,^{22a,22b} A. Gabrielli,¹⁶ G. P. Gach,^{41a} S. Gadatsch,³² S. Gadomski,⁸⁰ G. Gagliardi,^{53a,53b} L. G. Gagnon,⁹⁷ C. Galea,¹⁰⁸ B. Galhardo,^{128a,128c} E. J. Gallas,¹²² B. J. Gallop,¹³³ P. Gallus,¹³⁰ G. Galster,³⁹ K. K. Gan,¹¹³ S. Ganguly,³⁷ Y. Gao,⁷⁷ Y. S. Gao,^{145,h} F. M. Garay Walls,⁴⁹ C. García,¹⁷⁰ J. E. García Navarro,¹⁷⁰ J. A. García Pascual,^{35a} M. Garcia-Sciveres,¹⁶ R. W. Gardner,³³ N. Garelli,¹⁴⁵ V. Garonne,¹²¹ A. Gascon Bravo,⁴⁵ K. Gasnikova,⁴⁵ C. Gatti,⁵⁰ A. Gaudiello,^{53a,53b} G. Gaudio,^{123a} I. L. Gavrilenko,⁹⁸ C. Gay,¹⁷¹ G. Gaycken,²³ E. N. Gazis,¹⁰ C. N. P. Gee,¹³³ J. Geisen,⁵⁷ M. Geisen,⁸⁶ M. P. Geisler,^{60a} K. Gellerstedt,^{148a,148b} C. Gemme,^{53a} M. H. Genest,⁵⁸ C. Geng,⁹² S. Gentile,^{134a,134b} C. Gentsos,¹⁵⁶ S. George,⁸⁰ D. Gerbaudo,¹³ A. Gershon,¹⁵⁵ G. Geßner,⁴⁶ S. Ghasemi,¹⁴³ M. Ghneimat,²³ B. Giacobbe,^{22a} S. Giagu,^{134a,134b} P. Giannetti,^{126a,126b} S. M. Gibson,⁸⁰ M. Gignac,¹⁷¹ M. Gilchriese,¹⁶ D. Gillberg,³¹ G. Gilles,¹⁷⁸ D. M. Gingrich,^{3,e} N. Giokaris,^{9,a} M. P. Giordani,^{167a,167c} F. M. Giorgi,^{22a} P. F. Giraud,¹³⁸ P. Giromini,⁵⁹ D. Giugni,^{94a} F. Giuli,¹²² C. Giuliani,¹⁰³ M. Giulini,^{60b} B. K. Gjelsten,¹²¹ S. Gkaitatzis,¹⁵⁶ I. Gkialas,⁹ E. L. Gkoukousis,¹³⁹ P. Gkoutoumis,¹⁰ L. K. Gladilin,¹⁰¹ C. Glasman,⁸⁵ J. Glatzer,¹³ P. C. F. Glaysher,⁴⁵ A. Glazov,⁴⁵ M. Goblirsch-Kolb,²⁵ J. Godlewski,⁴² S. Goldfarb,⁹¹ T. Golling,⁵² D. Golubkov,¹³² A. Gomes,^{128a,128b,128d} R. Gonçalves,^{128a} R. Goncalves Gama,^{26a} J. Goncalves Pinto Firmino Da Costa,¹³⁸ G. Gonella,⁵¹ L. Gonella,¹⁹ A. Gongadze,⁶⁸ S. González de la Hoz,¹⁷⁰ S. Gonzalez-Sevilla,⁵² L. Goossens,³² P. A. Gorbounov,⁹⁹ H. A. Gordon,²⁷ I. Gorelov,¹⁰⁷ B. Gorini,³² E. Gorini,^{76a,76b} A. Gorišek,⁷⁸ A. T. Goshaw,⁴⁸ C. Gössling,⁴⁶ M. I. Gostkin,⁶⁸ C. A. Gottardo,²³ C. R. Goudet,¹¹⁹ D. Goujdami,^{137c} A. G. Goussiou,¹⁴⁰ N. Govender,^{147b,t} E. Gozani,¹⁵⁴ L. Graber,⁵⁷ I. Grabowska-Bold,^{41a} P. O. J. Gradin,¹⁶⁸ J. Gramling,¹⁶⁶ E. Gramstad,¹²¹ S. Grancagnolo,¹⁷ V. Gratchev,¹²⁵ P. M. Gravila,^{28f} C. Gray,⁵⁶ H. M. Gray,¹⁶ Z. D. Greenwood,^{82,u} C. Grefe,²³ K. Gregersen,⁸¹ I. M. Gregor,⁴⁵ P. Grenier,¹⁴⁵ K. Grevtsov,⁵ J. Griffiths,⁸ A. A. Grillo,¹³⁹ K. Grimm,⁷⁵

S. Grinstein,^{13,v} Ph. Gris,³⁷ J.-F. Grivaz,¹¹⁹ S. Groh,⁸⁶ E. Gross,¹⁷⁵ J. Grosse-Knetter,⁵⁷ G. C. Grossi,⁸² Z. J. Grout,⁸¹ A. Grummer,¹⁰⁷ L. Guan,⁹² W. Guan,¹⁷⁶ J. Guenther,⁶⁵ F. Guescini,^{163a} D. Guest,¹⁶⁶ O. Gueta,¹⁵⁵ B. Gui,¹¹³ E. Guido,^{53a,53b} T. Guillemain,⁵ S. Guindon,² U. Gul,⁵⁶ C. Gumpert,³² J. Guo,^{36c} W. Guo,⁹² Y. Guo,^{36a} R. Gupta,⁴³ S. Gupta,¹²² G. Gustavino,^{134a,134b} P. Gutierrez,¹¹⁵ N. G. Gutierrez Ortiz,⁸¹ C. Gutsche,⁸¹ C. Guyot,¹³⁸ M. P. Guzik,^{41a} C. Gwenlan,¹²² C. B. Gwilliam,⁷⁷ A. Haas,¹¹² C. Haber,¹⁶ H. K. Hadavand,⁸ N. Haddad,^{137e} A. Hadeef,⁸⁸ S. Hageböck,²³ M. Hagihara,¹⁶⁴ H. Hakobyan,^{180,a} M. Haleem,⁴⁵ J. Haley,¹¹⁶ G. Halladjian,⁹³ G. D. Hallewell,⁸⁸ K. Hamacher,¹⁷⁸ P. Hamal,¹¹⁷ K. Hamano,¹⁷² A. Hamilton,^{147a} G. N. Hamity,¹⁴¹ P. G. Hamnett,⁴⁵ L. Han,^{36a} S. Han,^{35a} K. Hanagaki,^{69,w} K. Hanawa,¹⁵⁷ M. Hance,¹³⁹ B. Haney,¹²⁴ R. Hankache,⁸³ P. Hanke,^{60a} J. B. Hansen,³⁹ J. D. Hansen,³⁹ M. C. Hansen,²³ P. H. Hansen,³⁹ K. Hara,¹⁶⁴ A. S. Hard,¹⁷⁶ T. Harenberg,¹⁷⁸ F. Hariri,¹¹⁹ S. Harkusha,⁹⁵ R. D. Harrington,⁴⁹ P. F. Harrison,¹⁷³ N. M. Hartmann,¹⁰² M. Hasegawa,⁷⁰ Y. Hasegawa,¹⁴² A. Hasib,⁴⁹ S. Hassani,¹³⁸ S. Haug,¹⁸ R. Hauser,⁹³ L. Hauswald,⁴⁷ L. B. Havener,³⁸ M. Havranek,¹³⁰ C. M. Hawkes,¹⁹ R. J. Hawkings,³² D. Hayakawa,¹⁵⁹ D. Hayden,⁹³ C. P. Hays,¹²² J. M. Hays,⁷⁹ H. S. Hayward,⁷⁷ S. J. Haywood,¹³³ S. J. Head,¹⁹ T. Heck,⁸⁶ V. Hedberg,⁸⁴ L. Heelan,⁸ K. K. Heidegger,⁵¹ S. Heim,⁴⁵ T. Heim,¹⁶ B. Heinemann,^{45,x} J. J. Heinrich,¹⁰² L. Heinrich,¹¹² C. Heinz,⁵⁵ J. Hejbal,¹²⁹ L. Helary,³² A. Held,¹⁷¹ S. Hellman,^{148a,148b} C. Hensens,³² R. C. W. Henderson,⁷⁵ Y. Heng,¹⁷⁶ S. Henkelmann,¹⁷¹ A. M. Henriques Correia,³² S. Henrot-Versille,¹¹⁹ G. H. Herbert,¹⁷ H. Herde,²⁵ V. Herget,¹⁷⁷ Y. Hernández Jiménez,^{147c} H. Herr,⁸⁶ G. Herten,⁵¹ R. Hertenberger,¹⁰² L. Hervas,³² T. C. Herwig,¹²⁴ G. G. Hesketh,⁸¹ N. P. Hessey,^{163a} J. W. Hetherly,⁴³ S. Higashino,⁶⁹ E. Higón-Rodríguez,¹⁷⁰ E. Hill,¹⁷² J. C. Hill,³⁰ K. H. Hiller,⁴⁵ S. J. Hillier,¹⁹ M. Hils,⁴⁷ I. Hinchliffe,¹⁶ M. Hirose,⁵¹ D. Hirschbuehl,¹⁷⁸ B. Hiti,⁷⁸ O. Hladik,¹²⁹ X. Hoad,⁴⁹ J. Hobbs,¹⁵⁰ N. Hod,^{163a} M. C. Hodgkinson,¹⁴¹ P. Hodgson,¹⁴¹ A. Hoecker,³² M. R. Hoferkamp,¹⁰⁷ F. Hoenig,¹⁰² D. Hohn,²³ T. R. Holmes,³³ M. Homann,⁴⁶ S. Honda,¹⁶⁴ T. Honda,⁶⁹ T. M. Hong,¹²⁷ B. H. Hooberman,¹⁶⁹ W. H. Hopkins,¹¹⁸ Y. Horii,¹⁰⁵ A. J. Horton,¹⁴⁴ J.-Y. Hostachy,⁵⁸ S. Hou,¹⁵³ A. Hoummada,^{137a} J. Howarth,⁸⁷ J. Hoya,⁷⁴ M. Hrabovsky,¹¹⁷ J. Hrdinka,³² I. Hristova,¹⁷ J. Hrivnac,¹¹⁹ T. Hryn'ova,⁵ A. Hrynevich,⁹⁶ P. J. Hsu,⁶³ S.-C. Hsu,¹⁴⁰ Q. Hu,^{36a} S. Hu,^{36c} Y. Huang,^{35a} Z. Hubacek,¹³⁰ F. Hubaut,⁸⁸ F. Huegging,²³ T. B. Huffman,¹²² E. W. Hughes,³⁸ G. Hughes,⁷⁵ M. Huhtinen,³² P. Huo,¹⁵⁰ N. Huseynov,^{68,c} J. Huston,⁹³ J. Huth,⁵⁹ G. Iacobucci,⁵² G. Iakovidis,²⁷ I. Ibragimov,¹⁴³ L. Iconomidou-Fayard,¹¹⁹ Z. Idrissi,^{137e} P. Iengo,³² O. Igonkina,^{109,y} T. Iizawa,¹⁷⁴ Y. Ikegami,⁶⁹ M. Ikeno,⁶⁹ Y. Ilchenko,^{11,z} D. Iliadis,¹⁵⁶ N. Ilic,¹⁴⁵ G. Introzzi,^{123a,123b} P. Ioannou,^{9,a} M. Iodice,^{136a} K. Iordanidou,³⁸ V. Ippolito,⁵⁹ M. F. Isacson,¹⁶⁸ N. Ishijima,¹²⁰ M. Ishino,¹⁵⁷ M. Ishitsuka,¹⁵⁹ C. Issever,¹²² S. Istin,^{20a} F. Ito,¹⁶⁴ J. M. Iturbe Ponce,⁸⁷ R. Iuppa,^{162a,162b} H. Iwasaki,⁶⁹ J. M. Izen,⁴⁴ V. Izzo,^{106a} S. Jabbar,³ P. Jackson,¹ R. M. Jacobs,²³ V. Jain,² K. B. Jakobi,⁸⁶ K. Jakobs,⁵¹ S. Jakobsen,⁶⁵ T. Jakoubek,¹²⁹ D. O. Jamin,¹¹⁶ D. K. Jana,⁸² R. Jansky,⁵² J. Janssen,²³ M. Janus,⁵⁷ P. A. Janus,^{41a} G. Jarlskog,⁸⁴ N. Javadov,^{68,c} T. Javůrek,⁵¹ M. Javurkova,⁵¹ F. Jeanneau,¹³⁸ L. Jeanty,¹⁶ J. Jejelava,^{54a,aa} A. Jelinskas,¹⁷³ P. Jenni,^{51,bb} C. Jeske,¹⁷³ S. Jézéquel,⁵ H. Ji,¹⁷⁶ J. Jia,¹⁵⁰ H. Jiang,⁶⁷ Y. Jiang,^{36a} Z. Jiang,¹⁴⁵ S. Jiggins,⁸¹ J. Jimenez Pena,¹⁷⁰ S. Jin,^{35a} A. Jinaru,^{28b} O. Jinnouchi,¹⁵⁹ H. Jivan,^{147c} P. Johansson,¹⁴¹ K. A. Johns,⁷ C. A. Johnson,⁶⁴ W. J. Johnson,¹⁴⁰ K. Jon-And,^{148a,148b} R. W. L. Jones,⁷⁵ S. D. Jones,¹⁵¹ S. Jones,⁷ T. J. Jones,⁷⁷ J. Jongmanns,^{60a} P. M. Jorge,^{128a,128b} J. Jovicevic,^{163a} X. Ju,¹⁷⁶ A. Juste Rozas,^{13,v} M. K. Köhler,¹⁷⁵ A. Kaczmarska,⁴² M. Kado,¹¹⁹ H. Kagan,¹¹³ M. Kagan,¹⁴⁵ S. J. Kahn,⁸⁸ T. Kaji,¹⁷⁴ E. Kajomovitz,⁴⁸ C. W. Kalderon,⁸⁴ A. Kaluza,⁸⁶ S. Kama,⁴³ A. Kamenshchikov,¹³² N. Kanaya,¹⁵⁷ L. Kanjir,⁷⁸ V. A. Kantserov,¹⁰⁰ J. Kanzaki,⁶⁹ B. Kaplan,¹¹² L. S. Kaplan,¹⁷⁶ D. Kar,^{147c} K. Karakostas,¹⁰ N. Karastathis,¹⁰ M. J. Kareem,⁵⁷ E. Karentzos,¹⁰ S. N. Karpov,⁶⁸ Z. M. Karpova,⁶⁸ K. Karthik,¹¹² V. Kartvelishvili,⁷⁵ A. N. Karyukhin,¹³² K. Kasahara,¹⁶⁴ L. Kashif,¹⁷⁶ R. D. Kass,¹¹³ A. Kastanas,¹⁴⁹ Y. Kataoka,¹⁵⁷ C. Kato,¹⁵⁷ A. Katre,⁵² J. Katzy,⁴⁵ K. Kawade,⁷⁰ K. Kawagoe,⁷³ T. Kawamoto,¹⁵⁷ G. Kawamura,⁵⁷ E. F. Kay,⁷⁷ V. F. Kazanin,^{111,d} R. Keeler,¹⁷² R. Kehoe,⁴³ J. S. Keller,³¹ J. J. Kempster,⁸⁰ J. Kendrick,¹⁹ H. Keoshkerian,¹⁶¹ O. Kepka,¹²⁹ B. P. Kerševan,⁷⁸ S. Kersten,¹⁷⁸ R. A. Keyes,⁹⁰ M. Khader,¹⁶⁹ F. Khalil-zada,¹² A. Khanov,¹¹⁶ A. G. Kharlamov,^{111,d} T. Kharlamova,^{111,d} A. Khodinov,¹⁶⁰ T. J. Khoo,⁵² V. Khovanskiy,^{99,a} E. Khramov,⁶⁸ J. Khubua,^{54b,cc} S. Kido,⁷⁰ C. R. Kilby,⁸⁰ H. Y. Kim,⁸ S. H. Kim,¹⁶⁴ Y. K. Kim,³³ N. Kimura,¹⁵⁶ O. M. Kind,¹⁷ B. T. King,⁷⁷ D. Kirchmeier,⁴⁷ J. Kirk,¹³³ A. E. Kiryunin,¹⁰³ T. Kishimoto,¹⁵⁷ D. Kisiielewska,^{41a} K. Kiuchi,¹⁶⁴ O. Kivernyk,⁵ E. Kladiva,^{146b} T. Klapdor-Kleingrothaus,⁵¹ M. H. Klein,³⁸ M. Klein,⁷⁷ U. Klein,⁷⁷ K. Kleinknecht,⁸⁶ P. Klimek,¹¹⁰ A. Klimentov,²⁷ R. Klingenberg,⁴⁶ T. Klingl,²³ T. Klioutchnikova,³² E.-E. Kluge,^{60a} P. Kluit,¹⁰⁹ S. Kluth,¹⁰³ E. Kneringer,⁶⁵ E. B. F. G. Knoop,⁸⁸ A. Knue,¹⁰³ A. Kobayashi,¹⁵⁷ D. Kobayashi,¹⁵⁹ T. Kobayashi,¹⁵⁷ M. Kobel,⁴⁷ M. Kocian,¹⁴⁵ P. Kodys,¹³¹ T. Koffas,³¹ E. Koffeman,¹⁰⁹ N. M. Köhler,¹⁰³ T. Koi,¹⁴⁵ M. Kolb,^{60b} I. Koletsou,⁵ A. A. Komar,^{98,a} Y. Komori,¹⁵⁷ T. Kondo,⁶⁹ N. Kondrashova,^{36c} K. Köneke,⁵¹ A. C. König,¹⁰⁸ T. Kono,^{69,dd} R. Konoplich,^{112,ee} N. Konstantinidis,⁸¹ R. Kopeliansky,⁶⁴ S. Koperny,^{41a} A. K. Kopp,⁵¹ K. Korcyl,⁴² K. Kordas,¹⁵⁶ A. Korn,⁸¹ A. A. Korol,^{111,d}

I. Korolkov,¹³ E. V. Korolkova,¹⁴¹ O. Kortner,¹⁰³ S. Kortner,¹⁰³ T. Kosek,¹³¹ V. V. Kostyukhin,²³ A. Kotwal,⁴⁸
A. Koulouris,¹⁰ A. Kourkoumeli-Charalampidi,^{123a,123b} C. Kourkoumelis,⁹ E. Kourlitis,¹⁴¹ V. Kouskoura,²⁷
A. B. Kowalewska,⁴² R. Kowalewski,¹⁷² T. Z. Kowalski,^{41a} C. Kozakai,¹⁵⁷ W. Kozanecki,¹³⁸ A. S. Kozhin,¹³²
V. A. Kramarenko,¹⁰¹ G. Kramberger,⁷⁸ D. Krasnoperstev,¹⁰⁰ M. W. Krasny,⁸³ A. Krasznahorkay,³² D. Krauss,¹⁰³
J. A. Kremer,^{41a} J. Kretschmar,⁷⁷ K. Kreutzfeldt,⁵⁵ P. Krieger,¹⁶¹ K. Krizka,³³ K. Kroeninger,⁴⁶ H. Kroha,¹⁰³ J. Kroll,¹²⁹
J. Kroll,¹²⁴ J. Kroseberg,²³ J. Krstic,¹⁴ U. Kruchonak,⁶⁸ H. Krüger,²³ N. Krumnack,⁶⁷ M. C. Kruse,⁴⁸ T. Kubota,⁹¹
H. Kucuk,⁸¹ S. Kudah,^{4b} J. T. Kuechler,¹⁷⁸ S. Kuehn,³² A. Kugel,^{60c} F. Kuger,¹⁷⁷ T. Kuhl,⁴⁵ V. Kukhtin,⁶⁸ R. Kukla,⁸⁸
Y. Kulchitsky,⁹⁵ S. Kuleshov,^{34b} Y. P. Kulinich,¹⁶⁹ M. Kuna,^{134a,134b} T. Kunigo,⁷¹ A. Kupco,¹²⁹ T. Kupfer,⁴⁶ O. Kuprash,¹⁵⁵
H. Kurashige,⁷⁰ L. L. Kurchaninov,^{163a} Y. A. Kurochkin,⁹⁵ M. G. Kurth,^{35a} V. Kus,¹²⁹ E. S. Kuwertz,¹⁷² M. Kuze,¹⁵⁹
J. Kvita,¹¹⁷ T. Kwan,¹⁷² D. Kyriazopoulos,¹⁴¹ A. La Rosa,¹⁰³ J. L. La Rosa Navarro,^{26d} L. La Rotonda,^{40a,40b} C. Lacasta,¹⁷⁰
F. Lacava,^{134a,134b} J. Lacey,⁴⁵ H. Lacker,¹⁷ D. Lacour,⁸³ E. Ladygin,⁶⁸ R. Lafaye,⁵ B. Laforge,⁸³ T. Lagouri,¹⁷⁹ S. Lai,⁵⁷
S. Lammers,⁶⁴ W. Lampl,⁷ E. Lançon,²⁷ U. Landgraf,⁵¹ M. P. J. Landon,⁷⁹ M. C. Lanfermann,⁵² V. S. Lang,^{60a} J. C. Lange,¹³
R. J. Langenberg,³² A. J. Lankford,¹⁶⁶ F. Lanni,²⁷ K. Lantzsck,²³ A. Lanza,^{123a} A. Lapertosa,^{53a,53b} S. Laplace,⁸³
J. F. Laporte,¹³⁸ T. Lari,^{94a} F. Lasagni Manghi,^{22a,22b} M. Lassnig,³² P. Laurelli,⁵⁰ W. Lavrijsen,¹⁶ A. T. Law,¹³⁹ P. Laycock,⁷⁷
T. Lazovich,⁵⁹ M. Lazzaroni,^{94a,94b} B. Le,⁹¹ O. Le Dortz,⁸³ E. Le Guirriec,⁸⁸ E. P. Le Quilleuc,¹³⁸ M. LeBlanc,¹⁷²
T. LeCompte,⁶ F. Ledroit-Guillon,⁵⁸ C. A. Lee,²⁷ G. R. Lee,^{133,ff} S. C. Lee,¹⁵³ L. Lee,⁵⁹ B. Lefebvre,⁹⁰ G. Lefebvre,⁸³
M. Lefebvre,¹⁷² F. Legger,¹⁰² C. Leggett,¹⁶ A. Lehan,⁷⁷ G. Lehmann Miotto,³² X. Lei,⁷ W. A. Leight,⁴⁵ M. A. L. Leite,^{26d}
R. Leitner,¹³¹ D. Lellouch,¹⁷⁵ B. Lemmer,⁵⁷ K. J. C. Leney,⁸¹ T. Lenz,²³ B. Lenzi,³² R. Leone,⁷ S. Leone,^{126a,126b}
C. Leonidopoulos,⁴⁹ G. Lerner,¹⁵¹ C. Leroy,⁹⁷ A. A. J. Lesage,¹³⁸ C. G. Lester,³⁰ M. Levchenko,¹²⁵ J. Levêque,⁵ D. Levin,⁹²
L. J. Levinson,¹⁷⁵ M. Levy,¹⁹ D. Lewis,⁷⁹ B. Li,^{36a,gg} C. Li,^{36a} H. Li,¹⁵⁰ L. Li,^{36c} Q. Li,^{35a} S. Li,⁴⁸ X. Li,^{36c} Y. Li,¹⁴³
Z. Liang,^{35a} B. Liberti,^{135a} A. Liblong,¹⁶¹ K. Lie,^{62c} J. Liebal,²³ W. Liebig,¹⁵ A. Limosani,¹⁵² S. C. Lin,¹⁸³ T. H. Lin,⁸⁶
B. E. Lindquist,¹⁵⁰ A. E. Lioni,⁵² E. Lipeles,¹²⁴ A. Lipniacka,¹⁵ M. Lisovsky,^{60b} T. M. Liss,¹⁶⁹ A. Lister,¹⁷¹ A. M. Litke,¹³⁹
B. Liu,^{153,hh} H. Liu,⁹² H. Liu,²⁷ J. K. K. Liu,¹²² J. Liu,^{36b} J. B. Liu,^{36a} K. Liu,⁸⁸ L. Liu,¹⁶⁹ M. Liu,^{36a} Y. L. Liu,^{36a} Y. Liu,^{36a}
M. Livan,^{123a,123b} A. Lleres,⁵⁸ J. Llorente Merino,^{35a} S. L. Lloyd,⁷⁹ C. Y. Lo,^{62b} F. Lo Sterzo,¹⁵³ E. M. Lobodzinska,⁴⁵
P. Loch,⁷ F. K. Loebinger,⁸⁷ A. Loesle,⁵¹ K. M. Loew,²⁵ A. Loginov,^{179,a} T. Lohse,¹⁷ K. Lohwasser,⁴⁵ M. Lokajicek,¹²⁹
B. A. Long,²⁴ J. D. Long,¹⁶⁹ R. E. Long,⁷⁵ L. Longo,^{76a,76b} K. A. Looper,¹¹³ J. A. Lopez,^{34b} D. Lopez Mateos,⁵⁹
I. Lopez Paz,¹³ A. Lopez Solis,⁸³ J. Lorenz,¹⁰² N. Lorenzo Martinez,⁵ M. Losada,²¹ P. J. Lösel,¹⁰² X. Lou,^{35a} A. Lounis,¹¹⁹
J. Love,⁶ P. A. Love,⁷⁵ H. Lu,^{62a} N. Lu,⁹² Y. J. Lu,⁶³ H. J. Lubatti,¹⁴⁰ C. Luci,^{134a,134b} A. Lucotte,⁵⁸ C. Luedtke,⁵¹
F. Luehring,⁶⁴ W. Lukas,⁶⁵ L. Luminari,^{134a} O. Lundberg,^{148a,148b} B. Lund-Jensen,¹⁴⁹ P. M. Luzi,⁸³ D. Lynn,²⁷ R. Lysak,¹²⁹
E. Lytken,⁸⁴ V. Lyubushkin,⁶⁸ H. Ma,²⁷ L. L. Ma,^{36b} Y. Ma,^{36b} G. Maccarrone,⁵⁰ A. Macchiolo,¹⁰³ C. M. Macdonald,¹⁴¹
B. Maček,⁷⁸ J. Machado Miguens,^{124,128b} D. Madaffari,⁸⁸ R. Madar,³⁷ W. F. Mader,⁴⁷ A. Madsen,⁴⁵ J. Maeda,⁷⁰
S. Maeland,¹⁵ T. Maeno,²⁷ A. S. Maevskiy,¹⁰¹ E. Magradze,⁵⁷ J. Mahlstedt,¹⁰⁹ C. Maiani,¹¹⁹ C. Maidantchik,^{26a}
A. A. Maier,¹⁰³ T. Maier,¹⁰² A. Maio,^{128a,128b,128d} O. Majersky,^{146a} S. Majewski,¹¹⁸ Y. Makida,⁶⁹ N. Makovec,¹¹⁹
B. Malaescu,⁸³ Pa. Malecki,⁴² V. P. Maleev,¹²⁵ F. Malek,⁵⁸ U. Mallik,⁶⁶ D. Malon,⁶ C. Malone,³⁰ S. Maltezos,¹⁰
S. Malyukov,³² J. Mamuzic,¹⁷⁰ G. Mancini,⁵⁰ L. Mandelli,^{94a} I. Mandić,⁷⁸ J. Maneira,^{128a,128b}
L. Manhaes de Andrade Filho,^{26b} J. Manjarres Ramos,⁴⁷ A. Mann,¹⁰² A. Manouos,³² B. Mansoulie,¹³⁸ J. D. Mansour,^{35a}
R. Mantifel,⁹⁰ M. Mantoani,⁵⁷ S. Manzoni,^{94a,94b} L. Mapelli,³² G. Marceca,²⁹ L. March,⁵² L. Marchese,¹²² G. Marchiori,⁸³
M. Marcisovsky,¹²⁹ M. Marjanovic,³⁷ D. E. Marley,⁹² F. Marroquim,^{26a} S. P. Marsden,⁸⁷ Z. Marshall,¹⁶
M. U. F. Martensson,¹⁶⁸ S. Marti-Garcia,¹⁷⁰ C. B. Martin,¹¹³ T. A. Martin,¹⁷³ V. J. Martin,⁴⁹ B. Martin dit Latour,¹⁵
M. Martinez,^{13,v} V. I. Martinez Outschoorn,¹⁶⁹ S. Martin-Haugh,¹³³ V. S. Martoiu,^{28b} A. C. Martyniuk,⁸¹ A. Marzin,³²
L. Masetti,⁸⁶ T. Mashimo,¹⁵⁷ R. Mashinistov,⁹⁸ J. Masik,⁸⁷ A. L. Maslennikov,^{111,d} L. Massa,^{135a,135b} P. Mastrandrea,⁵
A. Mastroberardino,^{40a,40b} T. Masubuchi,¹⁵⁷ P. Mättig,¹⁷⁸ J. Maurer,^{28b} S. J. Maxfield,⁷⁷ D. A. Maximov,^{111,d} R. Mazini,¹⁵³
I. Maznas,¹⁵⁶ S. M. Mazza,^{94a,94b} N. C. Mc Fadden,¹⁰⁷ G. Mc Goldrick,¹⁶¹ S. P. Mc Kee,⁹² A. McCarn,⁹² R. L. McCarthy,¹⁵⁰
T. G. McCarthy,¹⁰³ L. I. McClymont,⁸¹ E. F. McDonald,⁹¹ J. A. Mcfayden,⁸¹ G. Mchedlidze,⁵⁷ S. J. McMahan,¹³³
P. C. McNamara,⁹¹ R. A. McPherson,^{172,p} S. Meehan,¹⁴⁰ T. J. Megy,⁵¹ S. Mehlhase,¹⁰² A. Mehta,⁷⁷ T. Meideck,⁵⁸
K. Meier,^{60a} B. Meirose,⁴⁴ D. Melini,^{170,ii} B. R. Mellado Garcia,^{147c} J. D. Mellenthin,⁵⁷ M. Melo,^{146a} F. Meloni,¹⁸
S. B. Menary,⁸⁷ L. Meng,⁷⁷ X. T. Meng,⁹² A. Mengarelli,^{22a,22b} S. Menke,¹⁰³ E. Meoni,^{40a,40b} S. Mergelmeyer,¹⁷
P. Mermod,⁵² L. Merola,^{106a,106b} C. Meroni,^{94a} F. S. Merritt,³³ A. Messina,^{134a,134b} J. Metcalfe,⁶ A. S. Mete,¹⁶⁶ C. Meyer,¹²⁴
J-P. Meyer,¹³⁸ J. Meyer,¹⁰⁹ H. Meyer Zu Theenhausen,^{60a} F. Miano,¹⁵¹ R. P. Middleton,¹³³ S. Miglioranza,^{53a,53b} L. Mijović,⁴⁹

G. Mikenberg,¹⁷⁵ M. Mikestikova,¹²⁹ M. Mikuž,⁷⁸ M. Milesi,⁹¹ A. Milic,¹⁶¹ D. W. Miller,³³ C. Mills,⁴⁹ A. Milov,¹⁷⁵ D. A. Milstead,^{148a,148b} A. A. Minaenko,¹³² Y. Minami,¹⁵⁷ I. A. Minashvili,⁶⁸ A. I. Mincer,¹¹² B. Mindur,^{41a} M. Mineev,⁶⁸ Y. Minegishi,¹⁵⁷ Y. Ming,¹⁷⁶ L. M. Mir,¹³ K. P. Mistry,¹²⁴ T. Mitani,¹⁷⁴ J. Mitrevski,¹⁰² V. A. Mitsou,¹⁷⁰ A. Miucci,¹⁸ P. S. Miyagawa,¹⁴¹ A. Mizukami,⁶⁹ J. U. Mjörnmark,⁸⁴ T. Mkrtchyan,¹⁸⁰ M. Mlynarikova,¹³¹ T. Moa,^{148a,148b} K. Mochizuki,⁹⁷ P. Mogg,⁵¹ S. Mohapatra,³⁸ S. Molander,^{148a,148b} R. Moles-Valls,²³ R. Monden,⁷¹ M. C. Mondragon,⁹³ K. Mönig,⁴⁵ J. Monk,³⁹ E. Monnier,⁸⁸ A. Montalbano,¹⁵⁰ J. Montejo Berlingen,³² F. Monticelli,⁷⁴ S. Monzani,^{94a,94b} R. W. Moore,³ N. Morange,¹¹⁹ D. Moreno,²¹ M. Moreno Llácer,³² P. Morettini,^{53a} S. Morgenstern,³² D. Mori,¹⁴⁴ T. Mori,¹⁵⁷ M. Morii,⁵⁹ M. Morinaga,¹⁵⁷ V. Morisbak,¹²¹ A. K. Morley,¹⁵² G. Mornacchi,³² J. D. Morris,⁷⁹ L. Morvaj,¹⁵⁰ P. Moschovakos,¹⁰ M. Mosidze,^{54b} H. J. Moss,¹⁴¹ J. Moss,^{145,jj} K. Motohashi,¹⁵⁹ R. Mount,¹⁴⁵ E. Mountricha,²⁷ E. J. W. Moyse,⁸⁹ S. Muanza,⁸⁸ R. D. Mudd,¹⁹ F. Mueller,¹⁰³ J. Mueller,¹²⁷ R. S. P. Mueller,¹⁰² D. Muenstermann,⁷⁵ P. Mullen,⁵⁶ G. A. Mullier,¹⁸ F. J. Munoz Sanchez,⁸⁷ W. J. Murray,^{173,133} H. Musheghyan,¹⁸¹ M. Muškinja,⁷⁸ A. G. Myagkov,^{132,kk} M. Myska,¹³⁰ B. P. Nachman,¹⁶ O. Nackenhorst,⁵² K. Nagai,¹²² R. Nagai,^{69,dd} K. Nagano,⁶⁹ Y. Nagasaka,⁶¹ K. Nagata,¹⁶⁴ M. Nagel,⁵¹ E. Nagy,⁸⁸ A. M. Nairz,³² Y. Nakahama,¹⁰⁵ K. Nakamura,⁶⁹ T. Nakamura,¹⁵⁷ I. Nakano,¹¹⁴ R. F. Naranjo Garcia,⁴⁵ R. Narayan,¹¹ D. I. Narrias Villar,^{60a} I. Naryshkin,¹²⁵ T. Naumann,⁴⁵ G. Navarro,²¹ R. Nayyar,⁷ H. A. Neal,⁹² P. Yu. Nechaeva,⁹⁸ T. J. Neep,¹³⁸ A. Negri,^{123a,123b} M. Negrini,^{22a} S. Nektarijevic,¹⁰⁸ C. Nellist,¹¹⁹ A. Nelson,¹⁶⁶ M. E. Nelson,¹²² S. Nemecek,¹²⁹ P. Nemethy,¹¹² M. Nessi,^{32,ll} M. S. Neubauer,¹⁶⁹ M. Neumann,¹⁷⁸ P. R. Newman,¹⁹ T. Y. Ng,^{62c} T. Nguyen Manh,⁹⁷ R. B. Nickerson,¹²² R. Nicolaidou,¹³⁸ J. Nielsen,¹³⁹ V. Nikolaenko,^{132,kk} I. Nikolic-Audit,⁸³ K. Nikolopoulos,¹⁹ J. K. Nilsen,¹²¹ P. Nilsson,²⁷ Y. Ninomiya,¹⁵⁷ A. Nisati,^{134a} N. Nishu,^{35c} R. Nisius,¹⁰³ I. Nitsche,⁴⁶ T. Nobe,¹⁵⁷ Y. Noguchi,⁷¹ M. Nomachi,¹²⁰ I. Nomidis,³¹ M. A. Nomura,²⁷ T. Nooney,⁷⁹ M. Nordberg,³² N. Norjoharuddeen,¹²² O. Novgorodova,⁴⁷ S. Nowak,¹⁰³ M. Nozaki,⁶⁹ L. Nozka,¹¹⁷ K. Ntekas,¹⁶⁶ E. Nurse,⁸¹ F. Nuti,⁹¹ K. O'connor,²⁵ D. C. O'Neil,¹⁴⁴ A. A. O'Rourke,⁴⁵ V. O'Shea,⁵⁶ F. G. Oakham,^{31,e} H. Oberlack,¹⁰³ T. Obermann,²³ J. Ocariz,⁸³ A. Ochi,⁷⁰ I. Ochoa,³⁸ J. P. Ochoa-Ricoux,^{34a} S. Oda,⁷³ S. Odaka,⁶⁹ H. Ogren,⁶⁴ A. Oh,⁸⁷ S. H. Oh,⁴⁸ C. C. Ohm,¹⁶ H. Ohman,¹⁶⁸ H. Oide,^{53a,53b} H. Okawa,¹⁶⁴ Y. Okumura,¹⁵⁷ T. Okuyama,⁶⁹ A. Olariu,^{28b} L. F. Oleiro Seabra,^{128a} S. A. Olivares Pino,⁴⁹ D. Oliveira Damazio,²⁷ A. Olszewski,⁴² J. Olszowska,⁴² A. Onofre,^{128a,128e} K. Onogi,¹⁰⁵ P. U. E. Onyisi,^{11,z} M. J. Oreglia,³³ Y. Oren,¹⁵⁵ D. Orestano,^{136a,136b} N. Orlando,^{62b} R. S. Orr,¹⁶¹ B. Osculati,^{53a,53b,a} R. Ospanov,^{36a} G. Otero y Garzon,²⁹ H. Otono,⁷³ M. Ouchrif,^{137d} F. Ould-Saada,¹²¹ A. Ouraou,¹³⁸ K. P. Oussoren,¹⁰⁹ Q. Ouyang,^{35a} M. Owen,⁵⁶ R. E. Owen,¹⁹ V. E. Ozcan,^{20a} N. Ozturk,⁸ K. Pachal,¹⁴⁴ A. Pacheco Pages,¹³ L. Pacheco Rodriguez,¹³⁸ C. Padilla Aranda,¹³ S. Pagan Griso,¹⁶ M. Paganini,¹⁷⁹ F. Paige,²⁷ G. Palacino,⁶⁴ S. Palazzo,^{40a,40b} S. Palestini,³² M. Palka,^{41b} D. Pallin,³⁷ E. St. Panagiotopoulou,¹⁰ I. Panagoulas,¹⁰ C. E. Pandini,⁸³ J. G. Panduro Vazquez,⁸⁰ P. Pani,³² S. Panitkin,²⁷ D. Pantea,^{28b} L. Paolozzi,⁵² Th. D. Papadopoulou,¹⁰ K. Papageorgiou,⁹ A. Paramonov,⁶ D. Paredes Hernandez,¹⁷⁹ A. J. Parker,⁷⁵ M. A. Parker,³⁰ K. A. Parker,⁴⁵ F. Parodi,^{53a,53b} J. A. Parsons,³⁸ U. Parzefall,⁵¹ V. R. Pascuzzi,¹⁶¹ J. M. Pasner,¹³⁹ E. Pasqualucci,^{134a} S. Passaggio,^{53a} Fr. Pastore,⁸⁰ S. Patariaia,¹⁷⁸ J. R. Pater,⁸⁷ T. Pauly,³² B. Pearson,¹⁰³ S. Pedraza Lopez,¹⁷⁰ R. Pedro,^{128a,128b} S. V. Peleganchuk,^{111,d} O. Penc,¹²⁹ C. Peng,^{35a} H. Peng,^{36a} J. Penwell,⁶⁴ B. S. Peralva,^{26b} M. M. Perego,¹³⁸ D. V. Perepelitsa,²⁷ L. Perini,^{94a,94b} H. Pernegger,³² S. Perrella,^{106a,106b} R. Peschke,⁴⁵ V. D. Peshekhonov,^{68,a} K. Peters,⁴⁵ R. F. Y. Peters,⁸⁷ B. A. Petersen,³² T. C. Petersen,³⁹ E. Petit,⁵⁸ A. Petridis,¹ C. Petridou,¹⁵⁶ P. Petroff,¹¹⁹ E. Petrolo,^{134a} M. Petrov,¹²² F. Petrucci,^{136a,136b} N. E. Pettersson,⁸⁹ A. Peyaud,¹³⁸ R. Pezoa,^{34b} F. H. Phillips,⁹³ P. W. Phillips,¹³³ G. Piacquadio,¹⁵⁰ E. Pianori,¹⁷³ A. Picazio,⁸⁹ E. Piccaro,⁷⁹ M. A. Pickering,¹²² R. Piegaiia,²⁹ J. E. Pilcher,³³ A. D. Pilkington,⁸⁷ A. W. J. Pin,⁸⁷ M. Pinamonti,^{135a,135b} J. L. Pinfold,³ H. Pirumov,⁴⁵ M. Pitt,¹⁷⁵ L. Plazak,^{146a} M.-A. Pleier,²⁷ V. Pleskot,⁸⁶ E. Plotnikova,⁶⁸ D. Pluth,⁶⁷ P. Podberezko,¹¹¹ R. Poettgen,^{148a,148b} R. Poggi,^{123a,123b} L. Poggioli,¹¹⁹ D. Pohl,²³ G. Polesello,^{123a} A. Poley,⁴⁵ A. Policicchio,^{40a,40b} R. Polifka,³² A. Polini,^{22a} C. S. Pollard,⁵⁶ V. Polychronakos,²⁷ K. Pommès,³² D. Ponomarenko,¹⁰⁰ L. Pontecorvo,^{134a} B. G. Pope,⁹³ G. A. Popeneciu,^{28d} A. Poppleton,³² S. Pospisil,¹³⁰ K. Potamianos,¹⁶ I. N. Potrap,⁶⁸ C. J. Potter,³⁰ G. Poulard,³² T. Poulsen,⁸⁴ J. Poveda,³² M. E. Pozo Astigarraga,³² P. Pralavorio,⁸⁸ A. Pranko,¹⁶ S. Prell,⁶⁷ D. Price,⁸⁷ L. E. Price,⁶ M. Primavera,^{76a} S. Prince,⁹⁰ N. Proklova,¹⁰⁰ K. Prokofiev,^{62c} F. Prokoshin,^{34b} S. Protopopescu,²⁷ J. Proudfoot,⁶ M. Przybycien,^{41a} A. Puri,¹⁶⁹ P. Puzo,¹¹⁹ J. Qian,⁹² G. Qin,⁵⁶ Y. Qin,⁸⁷ A. Quadt,⁵⁷ M. Queitsch-Maitland,⁴⁵ D. Quilty,⁵⁶ S. Raddum,¹²¹ V. Radeka,²⁷ V. Radescu,¹²² S. K. Radhakrishnan,¹⁵⁰ P. Radloff,¹¹⁸ P. Rados,⁹¹ F. Ragusa,^{94a,94b} G. Rahal,¹⁸² J. A. Raine,⁸⁷ S. Rajagopalan,²⁷ C. Rangel-Smith,¹⁶⁸ T. Rashid,¹¹⁹ S. Raspopov,⁵ M. G. Ratti,^{94a,94b} D. M. Rauch,⁴⁵ F. Rauscher,¹⁰² S. Rave,⁸⁶ I. Ravinovich,¹⁷⁵ J. H. Rawling,⁸⁷ M. Raymond,³² A. L. Read,¹²¹ N. P. Readioff,⁵⁸ M. Reale,^{76a,76b} D. M. Rebuzzi,^{123a,123b} A. Redelbach,¹⁷⁷ G. Redlinger,²⁷ R. Reece,¹³⁹ R. G. Reed,^{147c} K. Reeves,⁴⁴ L. Rehnisch,¹⁷ J. Reichert,¹²⁴ A. Reiss,⁸⁶

C. Rembser,³² H. Ren,^{35a} M. Rescigno,^{134a} S. Resconi,^{94a} E. D. Resseguie,¹²⁴ S. Rettie,¹⁷¹ E. Reynolds,¹⁹
O. L. Rezanova,^{111,d} P. Reznicek,¹³¹ R. Rezvani,⁹⁷ R. Richter,¹⁰³ S. Richter,⁸¹ E. Richter-Was,^{41b} O. Ricken,²³ M. Ridel,⁸³
P. Rieck,¹⁰³ C. J. Riegel,¹⁷⁸ J. Rieger,⁵⁷ O. Rifki,¹¹⁵ M. Rijssenbeek,¹⁵⁰ A. Rimoldi,^{123a,123b} M. Rimoldi,¹⁸ L. Rinaldi,^{22a}
G. Ripellino,¹⁴⁹ B. Ristić,³² E. Ritsch,³² I. Riu,¹³ F. Rizatdinova,¹¹⁶ E. Rizvi,⁷⁹ C. Rizzi,¹³ R. T. Roberts,⁸⁷
S. H. Robertson,^{90,p} A. Robichaud-Veronneau,⁹⁰ D. Robinson,³⁰ J. E. M. Robinson,⁴⁵ A. Robson,⁵⁶ E. Rocco,⁸⁶
C. Roda,^{126a,126b} Y. Rodina,^{88,mm} S. Rodriguez Bosca,¹⁷⁰ A. Rodriguez Perez,¹³ D. Rodriguez Rodriguez,¹⁷⁰ S. Roe,³²
C. S. Rogan,⁵⁹ O. Røhne,¹²¹ J. Roloff,⁵⁹ A. Romaniouk,¹⁰⁰ M. Romano,^{22a,22b} S. M. Romano Saez,³⁷ E. Romero Adam,¹⁷⁰
N. Rompotis,⁷⁷ M. Ronzani,⁵¹ L. Roos,⁸³ S. Rosati,^{134a} K. Rosbach,⁵¹ P. Rose,¹³⁹ N.-A. Rosien,⁵⁷ E. Rossi,^{106a,106b}
L. P. Rossi,^{53a} J. H. N. Rosten,³⁰ R. Rosten,¹⁴⁰ M. Rotaru,^{28b} I. Roth,¹⁷⁵ J. Rothberg,¹⁴⁰ D. Rousseau,¹¹⁹ A. Rozanov,⁸⁸
Y. Rozen,¹⁵⁴ X. Ruan,^{147c} F. Rubbo,¹⁴⁵ F. Rühr,⁵¹ A. Ruiz-Martinez,³¹ Z. Rurikova,⁵¹ N. A. Rusakovich,⁶⁸ H. L. Russell,⁹⁰
J. P. Rutherford,⁷ N. Ruthmann,³² Y. F. Ryabov,¹²⁵ M. Rybar,¹⁶⁹ G. Rybkin,¹¹⁹ S. Ryu,⁶ A. Ryzhov,¹³² G. F. Rzehorz,⁵⁷
A. F. Saavedra,¹⁵² G. Sabato,¹⁰⁹ S. Sacerdoti,²⁹ H. F.-W. Sadrozinski,¹³⁹ R. Sadykov,⁶⁸ F. Safai Tehrani,^{134a} P. Saha,¹¹⁰
M. Sahinsoy,^{60a} M. Saimpert,⁴⁵ M. Saito,¹⁵⁷ T. Saito,¹⁵⁷ H. Sakamoto,¹⁵⁷ Y. Sakurai,¹⁷⁴ G. Salamanna,^{136a,136b}
J. E. Salazar Loyola,^{34b} D. Salek,¹⁰⁹ P. H. Sales De Bruin,¹⁶⁸ D. Salihagic,¹⁰³ A. Salmikov,¹⁴⁵ J. Salt,¹⁷⁰ D. Salvatore,^{40a,40b}
F. Salvatore,¹⁵¹ A. Salvucci,^{62a,62b,62c} A. Salzburger,³² D. Sammel,⁵¹ D. Sampsonidis,¹⁵⁶ D. Sampsonidou,¹⁵⁶ J. Sánchez,¹⁷⁰
V. Sanchez Martinez,¹⁷⁰ A. Sanchez Pineda,^{167a,167c} H. Sandaker,¹²¹ R. L. Sandbach,⁷⁹ C. O. Sander,⁴⁵ M. Sandhoff,¹⁷⁸
C. Sandoval,²¹ D. P. C. Sankey,¹³³ M. Sannino,^{53a,53b} Y. Sano,¹⁰⁵ A. Sansoni,⁵⁰ C. Santoni,³⁷ R. Santonico,^{135a,135b}
H. Santos,^{128a} I. Santoyo Castillo,¹⁵¹ A. Sapronov,⁶⁸ J. G. Saraiva,^{128a,128d} B. Sarrazin,²³ O. Sasaki,⁶⁹ K. Sato,¹⁶⁴ E. Sauvan,⁵
G. Savage,⁸⁰ P. Savard,^{161,e} N. Savic,¹⁰³ C. Sawyer,¹³³ L. Sawyer,^{82,u} J. Saxon,³³ C. Sbarra,^{22a} A. Sbrizzi,^{22a,22b} T. Scanlon,⁸¹
D. A. Scannicchio,¹⁶⁶ M. Scarcella,¹⁵² V. Scarfone,^{40a,40b} J. Schaarschmidt,¹⁴⁰ P. Schacht,¹⁰³ B. M. Schachtner,¹⁰²
D. Schaefer,³² L. Schaefer,¹²⁴ R. Schaefer,⁴⁵ J. Schaeffer,⁸⁶ S. Schaepe,²³ S. Schaezel,^{60b} U. Schäfer,⁸⁶ A. C. Schaffer,¹¹⁹
D. Schaile,¹⁰² R. D. Schamberger,¹⁵⁰ V. Scharf,^{60a} V. A. Schegelsky,¹²⁵ D. Scheirich,¹³¹ M. Schernau,¹⁶⁶ C. Schiavi,^{53a,53b}
S. Schier,¹³⁹ L. K. Schildgen,²³ C. Schillo,⁵¹ M. Schioppa,^{40a,40b} S. Schlenker,³² K. R. Schmidt-Sommerfeld,¹⁰³
K. Schmieden,³² C. Schmitt,⁸⁶ S. Schmitt,⁴⁵ S. Schmitz,⁸⁶ U. Schnoor,⁵¹ L. Schoeffel,¹³⁸ A. Schoening,^{60b}
B. D. Schoenrock,⁹³ E. Schopf,²³ M. Schott,⁸⁶ J. F. P. Schouwenberg,¹⁰⁸ J. Schovancova,¹⁸¹ S. Schramm,⁵² N. Schuh,⁸⁶
A. Schulte,⁸⁶ M. J. Schultens,²³ H.-C. Schultz-Coulon,^{60a} H. Schulz,¹⁷ M. Schumacher,⁵¹ B. A. Schumm,¹³⁹ Ph. Schune,¹³⁸
A. Schwartzman,¹⁴⁵ T. A. Schwarz,⁹² H. Schweiger,⁸⁷ Ph. Schwemling,¹³⁸ R. Schwienhorst,⁹³ J. Schwindling,¹³⁸
A. Sciandra,²³ G. Sciolla,²⁵ F. Scuri,^{126a,126b} F. Scutti,⁹¹ J. Searcy,⁹² P. Seema,²³ S. C. Seidel,¹⁰⁷ A. Seiden,¹³⁹ J. M. Seixas,^{26a}
G. Sekhniaidze,^{106a} K. Sekhon,⁹² S. J. Sekula,⁴³ N. Semprini-Cesari,^{22a,22b} S. Senkin,³⁷ C. Serfon,¹²¹ L. Serin,¹¹⁹
L. Serkin,^{167a,167b} M. Sessa,^{136a,136b} R. Seuster,¹⁷² H. Severini,¹¹⁵ T. Sfiligoj,⁷⁸ F. Sforza,³² A. Sfyrla,⁵² E. Shabalina,⁵⁷
N. W. Shaikh,^{148a,148b} L. Y. Shan,^{35a} R. Shang,¹⁶⁹ J. T. Shank,²⁴ M. Shapiro,¹⁶ P. B. Shatalov,⁹⁹ K. Shaw,^{167a,167b}
S. M. Shaw,⁸⁷ A. Shcherbakova,^{148a,148b} C. Y. Shehu,¹⁵¹ Y. Shen,¹¹⁵ N. Sherafati,³¹ P. Sherwood,⁸¹ L. Shi,^{153,nn} S. Shimizu,⁷⁰
C. O. Shimmin,¹⁷⁹ M. Shimojima,¹⁰⁴ I. P. J. Shipsey,¹²² S. Shirabe,⁷³ M. Shiyakova,^{68,oo} J. Shlomi,¹⁷⁵ A. Shmeleva,⁹⁸
D. Shoaleh Saadi,⁹⁷ M. J. Shochet,³³ S. Shojaii,^{94a} D. R. Shope,¹¹⁵ S. Shrestha,¹¹³ E. Shulga,¹⁰⁰ M. A. Shupe,⁷ P. Sicho,¹²⁹
A. M. Sickles,¹⁶⁹ P. E. Sidebo,¹⁴⁹ E. Sideras Haddad,^{147c} O. Sidiropoulou,¹⁷⁷ A. Sidoti,^{22a,22b} F. Siegert,⁴⁷ Dj. Sijacki,¹⁴
J. Silva,^{128a,128d} S. B. Silverstein,^{148a} V. Simak,¹³⁰ Lj. Simic,¹⁴ S. Simion,¹¹⁹ E. Simioni,⁸⁶ B. Simmons,⁸¹ M. Simon,⁸⁶
P. Sinervo,¹⁶¹ N. B. Sinev,¹¹⁸ M. Sioli,^{22a,22b} G. Siragusa,¹⁷⁷ I. Siral,⁹² S. Yu. Sivoklov,¹⁰¹ J. Sjölin,^{148a,148b} M. B. Skinner,⁷⁵
P. Skubic,¹¹⁵ M. Slater,¹⁹ T. Slavicek,¹³⁰ M. Slawinska,⁴² K. Sliwa,¹⁶⁵ R. Slovak,¹³¹ V. Smakhtin,¹⁷⁵ B. H. Smart,⁵
J. Smiesko,^{146a} N. Smirnov,¹⁰⁰ S. Yu. Smirnov,¹⁰⁰ Y. Smirnov,¹⁰⁰ L. N. Smirnova,^{101,pp} O. Smirnova,⁸⁴ J. W. Smith,⁵⁷
M. N. K. Smith,³⁸ R. W. Smith,³⁸ M. Smizanska,⁷⁵ K. Smolek,¹³⁰ A. A. Snesev,⁹⁸ I. M. Snyder,¹¹⁸ S. Snyder,²⁷
R. Sobie,^{172,p} F. Socher,⁴⁷ A. Soffer,¹⁵⁵ D. A. Soh,¹⁵³ G. Sokhrany,⁷⁸ C. A. Solans Sanchez,³² M. Solar,¹³⁰
E. Yu. Soldatov,¹⁰⁰ U. Soldevila,¹⁷⁰ A. A. Solodkov,¹³² A. Soloshenko,⁶⁸ O. V. Solovyanov,¹³² V. Solovyev,¹²⁵ P. Sommer,⁵¹
H. Son,¹⁶⁵ A. Sopczak,¹³⁰ D. Sosa,^{60b} C. L. Sotiropoulou,^{126a,126b} R. Soualah,^{167a,167c} A. M. Soukharev,^{111,d} D. South,⁴⁵
B. C. Sowden,⁸⁰ S. Spagnolo,^{76a,76b} M. Spalla,^{126a,126b} M. Spangenberg,¹⁷³ F. Spanò,⁸⁰ D. Sperlich,¹⁷ F. Spettel,¹⁰³
T. M. Spieker,^{60a} R. Spighi,^{22a} G. Spigo,³² L. A. Spiller,⁹¹ M. Spousta,¹³¹ R. D. St. Denis,^{56a} A. Stabile,^{94a} R. Stamen,^{60a}
S. Stamm,¹⁷ E. Stanecka,⁴² R. W. Staneck,⁶ C. Stanescu,^{136a} M. M. Stanitzki,⁴⁵ B. S. Stapf,¹⁰⁹ S. Stapnes,¹²¹
E. A. Starchenko,¹³² G. H. Stark,³³ J. Stark,⁵⁸ S. H. Stark,³⁹ P. Staroba,¹²⁹ P. Starovoitov,^{60a} S. Stärz,³² R. Staszewski,⁴²
P. Steinberg,²⁷ B. Stelzer,¹⁴⁴ H. J. Stelzer,³² O. Stelzer-Chilton,^{163a} H. Stenzel,⁵⁵ G. A. Stewart,⁵⁶ M. C. Stockton,¹¹⁸
M. Stoebe,⁹⁰ G. Stoicea,^{28b} P. Stolte,⁵⁷ S. Stonjek,¹⁰³ A. R. Stradling,⁸ A. Straessner,⁴⁷ M. E. Stramaglia,¹⁸ J. Strandberg,¹⁴⁹

S. Strandberg,^{148a,148b} M. Strauss,¹¹⁵ P. Strizenec,^{146b} R. Ströhrmer,¹⁷⁷ D. M. Strom,¹¹⁸ R. Stroynowski,⁴³ A. Strubig,¹⁰⁸ S. A. Stucci,²⁷ B. Stugu,¹⁵ N. A. Styles,⁴⁵ D. Su,¹⁴⁵ J. Su,¹²⁷ S. Suchek,^{60a} Y. Sugaya,¹²⁰ M. Suk,¹³⁰ V. V. Sulin,⁹⁸ DMS Sultan,^{162a,162b} S. Sultansoy,^{4c} T. Sumida,⁷¹ S. Sun,⁵⁹ X. Sun,³ K. Suruliz,¹⁵¹ C. J. E. Suster,¹⁵² M. R. Sutton,¹⁵¹ S. Suzuki,⁶⁹ M. Svatos,¹²⁹ M. Swiatlowski,³³ S. P. Swift,² I. Sykora,^{146a} T. Sykora,¹³¹ D. Ta,⁵¹ K. Tackmann,⁴⁵ J. Taenzer,¹⁵⁵ A. Taffard,¹⁶⁶ R. Tafirout,^{163a} N. Taiblum,¹⁵⁵ H. Takai,²⁷ R. Takashima,⁷² E. H. Takasugi,¹⁰³ T. Takeshita,¹⁴² Y. Takubo,⁶⁹ M. Talby,⁸⁸ A. A. Talyshev,^{111,d} J. Tanaka,¹⁵⁷ M. Tanaka,¹⁵⁹ R. Tanaka,¹¹⁹ S. Tanaka,⁶⁹ R. Tanioka,⁷⁰ B. B. Tannenwald,¹¹³ S. Tapia Araya,^{34b} S. Tapprogge,⁸⁶ S. Tarem,¹⁵⁴ G. F. Tartarelli,^{94a} P. Tas,¹³¹ M. Tasevsky,¹²⁹ T. Tashiro,⁷¹ E. Tassi,^{40a,40b} A. Tavares Delgado,^{128a,128b} Y. Tayalati,^{137e} A. C. Taylor,¹⁰⁷ G. N. Taylor,⁹¹ P. T. E. Taylor,⁹¹ W. Taylor,^{163b} P. Teixeira-Dias,⁸⁰ D. Temple,¹⁴⁴ H. Ten Kate,³² P. K. Teng,¹⁵³ J. J. Teoh,¹²⁰ F. Tepel,¹⁷⁸ S. Terada,⁶⁹ K. Terashi,¹⁵⁷ J. Terron,⁸⁵ S. Terzo,¹³ M. Testa,⁵⁰ R. J. Teuscher,^{161,p} T. Theveneaux-Pelzer,⁸⁸ J. P. Thomas,¹⁹ J. Thomas-Wilsker,⁸⁰ P. D. Thompson,¹⁹ A. S. Thompson,⁵⁶ L. A. Thomsen,¹⁷⁹ E. Thomson,¹²⁴ M. J. Tibbetts,¹⁶ R. E. Ticse Torres,⁸⁸ V. O. Tikhomirov,^{98,qq} Yu. A. Tikhonov,^{111,d} S. Timoshenko,¹⁰⁰ P. Tipton,¹⁷⁹ S. Tisserant,⁸⁸ K. Todome,¹⁵⁹ S. Todorova-Nova,⁵ J. Tojo,⁷³ S. Tokár,^{146a} K. Tokushuku,⁶⁹ E. Tolley,⁵⁹ L. Tomlinson,⁸⁷ M. Tomoto,¹⁰⁵ L. Tompkins,^{145,rr} K. Toms,¹⁰⁷ B. Tong,⁵⁹ P. Tornambe,⁵¹ E. Torrence,¹¹⁸ H. Torres,¹⁴⁴ E. Torró Pastor,¹⁴⁰ J. Toth,^{88,ss} F. Touchard,⁸⁸ D. R. Tovey,¹⁴¹ C. J. Treado,¹¹² T. Trefzger,¹⁷⁷ F. Tresoldi,¹⁵¹ A. Tricoli,²⁷ I. M. Trigger,^{163a} S. Trincaz-Duvoid,⁸³ M. F. Tripiana,¹³ W. Trischuk,¹⁶¹ B. Trocmé,⁵⁸ A. Trofymov,⁴⁵ C. Troncon,^{94a} M. Trotter-McDonald,¹⁶ M. Trovatelli,¹⁷² L. Truong,^{167a,167c} M. Trzebinski,⁴² A. Trzupek,⁴² K. W. Tsang,^{62a} J. C.-L. Tseng,¹²² P. V. Tsiarehka,⁹⁵ G. Tsipolitis,¹⁰ N. Tsirintanis,⁹ S. Tsiskaridze,¹³ V. Tsiskaridze,⁵¹ E. G. Tskhadadze,^{54a} K. M. Tsui,^{62a} I. I. Tsukerman,⁹⁹ V. Tsulaia,¹⁶ S. Tsuno,⁶⁹ D. Tsybychev,¹⁵⁰ Y. Tu,^{62b} A. Tudorache,^{28b} V. Tudorache,^{28b} T. T. Tulbure,^{28a} A. N. Tuna,⁵⁹ S. A. Tuppuri,^{22a,22b} S. Turchikhin,⁶⁸ D. Turgeman,¹⁷⁵ I. Turk Cakir,^{4b,tt} R. Turra,^{94a} P. M. Tuts,³⁸ G. Uccielli,^{22a,22b} I. Ueda,⁶⁹ M. Ughetto,^{148a,148b} F. Ukegawa,¹⁶⁴ G. Unal,³² A. Undrus,²⁷ G. Unel,¹⁶⁶ F. C. Ungaro,⁹¹ Y. Unno,⁶⁹ C. Unverdorben,¹⁰² J. Urban,^{146b} P. Urquijo,⁹¹ P. Urrejola,⁸⁶ G. Usai,⁸ J. Usui,⁶⁹ L. Vacavant,⁸⁸ V. Vacek,¹³⁰ B. Vachon,⁹⁰ C. Valderanis,¹⁰² E. Valdes Santurio,^{148a,148b} S. Valentinetti,^{22a,22b} A. Valero,¹⁷⁰ L. Valéry,¹³ S. Valkar,¹³¹ A. Vallier,⁵ J. A. Valls Ferrer,¹⁷⁰ W. Van Den Wollenberg,¹⁰⁹ H. van der Graaf,¹⁰⁹ P. van Gemmeren,⁶ J. Van Nieuwkoop,¹⁴⁴ I. van Vulpen,¹⁰⁹ M. C. van Woerden,¹⁰⁹ M. Vanadia,^{135a,135b} W. Vandelli,³² A. Vaniachine,¹⁶⁰ P. Vankov,¹⁰⁹ G. Vardanyan,¹⁸⁰ R. Vari,^{134a} E. W. Varnes,⁷ C. Varni,^{53a,53b} T. Varol,⁴³ D. Varouchas,¹¹⁹ A. Vartapetian,⁸ K. E. Varvell,¹⁵² J. G. Vasquez,¹⁷⁹ G. A. Vasquez,^{34b} F. Vazeille,³⁷ T. Vazquez Schroeder,⁹⁰ J. Veatch,⁵⁷ V. Veeraraghavan,⁷ L. M. Veloce,¹⁶¹ F. Veloso,^{128a,128c} S. Veneziano,^{134a} A. Ventura,^{76a,76b} M. Venturi,¹⁷² N. Venturi,³² A. Venturini,²⁵ V. Vercesi,^{123a} M. Verducci,^{136a,136b} W. Verkerke,¹⁰⁹ A. T. Vermeulen,¹⁰⁹ J. C. Vermeulen,¹⁰⁹ M. C. Vetterli,^{144,e} N. Viaux Maira,^{34b} O. Viazlo,⁸⁴ I. Vichou,^{169,a} T. Vickey,¹⁴¹ O. E. Vickey Boeriu,¹⁴¹ G. H. A. Viehhauser,¹²² S. Viel,¹⁶ L. Vigani,¹²² M. Villa,^{22a,22b} M. Villaplana Perez,^{94a,94b} E. Vilucchi,⁵⁰ M. G. Vincter,³¹ V. B. Vinogradov,⁶⁸ A. Vishwakarma,⁴⁵ C. Vittori,^{22a,22b} I. Vivarelli,¹⁵¹ S. Vlachos,¹⁰ M. Vogel,¹⁷⁸ P. Vokac,¹³⁰ G. Volpi,^{126a,126b} H. von der Schmitt,¹⁰³ E. von Toerne,²³ V. Vorobel,¹³¹ K. Vorobev,¹⁰⁰ M. Vos,¹⁷⁰ R. Voss,³² J. H. Vossebeld,⁷⁷ N. Vranjes,¹⁴ M. Vranjes Milosavljevic,¹⁴ V. Vrba,¹³⁰ M. Vreeswijk,¹⁰⁹ R. Vuillermet,³² I. Vukotic,³³ P. Wagner,²³ W. Wagner,¹⁷⁸ J. Wagner-Kuhr,¹⁰² H. Wahlberg,⁷⁴ S. Wahrmund,⁴⁷ J. Wakabayashi,¹⁰⁵ J. Walder,⁷⁵ R. Walker,¹⁰² W. Walkowiak,¹⁴³ V. Wallangen,^{148a,148b} C. Wang,^{35b} C. Wang,^{36b,uu} F. Wang,¹⁷⁶ H. Wang,¹⁶ H. Wang,³ J. Wang,⁴⁵ J. Wang,¹⁵² Q. Wang,¹¹⁵ R. Wang,⁶ S. M. Wang,¹⁵³ T. Wang,³⁸ W. Wang,^{153,vv} W. Wang,^{36a} Z. Wang,^{36c} C. Wantayaraj,¹¹⁸ A. Warburton,⁹⁰ C. P. Ward,³⁰ D. R. Wardrope,⁸¹ A. Washbrook,⁴⁹ P. M. Watkins,¹⁹ A. T. Watson,¹⁹ M. F. Watson,¹⁹ G. Watts,¹⁴⁰ S. Watts,⁸⁷ B. M. Waugh,⁸¹ A. F. Webb,¹¹ S. Webb,⁸⁶ M. S. Weber,¹⁸ S. W. Weber,¹⁷⁷ S. A. Weber,³¹ J. S. Webster,⁶ A. R. Weidberg,¹²² B. Weinert,⁶⁴ J. Weingarten,⁵⁷ M. Weirich,⁸⁶ C. Weiser,⁵¹ H. Weits,¹⁰⁹ P. S. Wells,³² T. Wenaus,²⁷ T. Wengler,³² S. Wenig,³² N. Wermes,²³ M. D. Werner,⁶⁷ P. Werner,³² M. Wessels,^{60a} K. Whalen,¹¹⁸ N. L. Whallon,¹⁴⁰ A. M. Wharton,⁷⁵ A. S. White,⁹² A. White,⁸ M. J. White,¹ R. White,^{34b} D. Whiteson,¹⁶⁶ B. W. Whitmore,⁷⁵ F. J. Wickens,¹³³ W. Wiedenmann,¹⁷⁶ M. Wielers,¹³³ C. Wigglesworth,³⁹ L. A. M. Wiik-Fuchs,²³ A. Wildauer,¹⁰³ F. Wilk,⁸⁷ H. G. Wilkens,³² H. H. Williams,¹²⁴ S. Williams,¹⁰⁹ C. Willis,⁹³ S. Willocq,⁸⁹ J. A. Wilson,¹⁹ I. Wingerter-Seez,⁵ E. Winkels,¹⁵¹ F. Winklmeier,¹¹⁸ O. J. Winston,¹⁵¹ B. T. Winter,²³ M. Wittgen,¹⁴⁵ M. Wobisch,^{82,u} T. M. H. Wolf,¹⁰⁹ R. Wolff,⁸⁸ M. W. Wolter,⁴² H. Wolters,^{128a,128c} V. W. S. Wong,¹⁷¹ S. D. Worm,¹⁹ B. K. Wosiek,⁴² J. Wotschack,³² K. W. Wozniak,⁴² M. Wu,³³ S. L. Wu,¹⁷⁶ X. Wu,⁵² Y. Wu,⁹² T. R. Wyatt,⁸⁷ B. M. Wynne,⁴⁹ S. Xella,³⁹ Z. Xi,⁹² L. Xia,^{35c} D. Xu,^{35a} L. Xu,²⁷ B. Yabsley,¹⁵² S. Yacoub,^{147a} D. Yamaguchi,¹⁵⁹ Y. Yamaguchi,¹²⁰ A. Yamamoto,⁶⁹ S. Yamamoto,¹⁵⁷ T. Yamanaka,¹⁵⁷ M. Yamatani,¹⁵⁷ K. Yamauchi,¹⁰⁵ Y. Yamazaki,⁷⁰ Z. Yan,²⁴ H. Yang,^{36c} H. Yang,¹⁶ Y. Yang,¹⁵³ Z. Yang,¹⁵ W.-M. Yao,¹⁶ Y. C. Yap,⁸³ Y. Yasu,⁶⁹ E. Yatsenko,⁵

K. H. Yau Wong,²³ J. Ye,⁴³ S. Ye,²⁷ I. Yeletsikh,⁶⁸ E. Yigitbasi,²⁴ E. Yildirim,⁸⁶ K. Yorita,¹⁷⁴ K. Yoshihara,¹²⁴ C. Young,¹⁴⁵ C. J. S. Young,³² J. Yu,⁸ J. Yu,⁶⁷ S. P. Y. Yuen,²³ I. Yusuff,^{30,ww} B. Zabinski,⁴² G. Zacharis,¹⁰ R. Zaidan,¹³ A. M. Zaitsev,^{132,kk} N. Zakharchuk,⁴⁵ J. Zalieckas,¹⁵ A. Zaman,¹⁵⁰ S. Zambito,⁵⁹ D. Zanzi,⁹¹ C. Zeitnitz,¹⁷⁸ G. Zemaityte,¹²² A. Zemla,^{41a} J. C. Zeng,¹⁶⁹ Q. Zeng,¹⁴⁵ O. Zenin,¹³² T. Ženiš,^{146a} D. Zerwas,¹¹⁹ D. Zhang,^{36b} D. Zhang,⁹² F. Zhang,¹⁷⁶ G. Zhang,^{36a,xx} H. Zhang,^{35b} J. Zhang,⁶ L. Zhang,⁵¹ L. Zhang,^{36a} M. Zhang,¹⁶⁹ P. Zhang,^{35b} R. Zhang,²³ R. Zhang,^{36a,uu} X. Zhang,^{36b} Y. Zhang,^{35a} Z. Zhang,¹¹⁹ X. Zhao,⁴³ Y. Zhao,^{36b,yy} Z. Zhao,^{36a} A. Zhemchugov,⁶⁸ B. Zhou,⁹² C. Zhou,¹⁷⁶ L. Zhou,⁴³ M. Zhou,^{35a} M. Zhou,¹⁵⁰ N. Zhou,^{35c} C. G. Zhu,^{36b} H. Zhu,^{35a} J. Zhu,⁹² Y. Zhu,^{36a} X. Zhuang,^{35a} K. Zhukov,⁹⁸ A. Zibell,¹⁷⁷ D. Zieminska,⁶⁴ N. I. Zimine,⁶⁸ C. Zimmermann,⁸⁶ S. Zimmermann,⁵¹ Z. Zinonos,¹⁰³ M. Zinser,⁸⁶ M. Ziolkowski,¹⁴³ L. Živković,¹⁴ G. Zobernig,¹⁷⁶ A. Zoccoli,^{22a,22b} R. Zou,³³ M. zur Nedden,¹⁷ and L. Zwalinski³²

(ATLAS Collaboration)

¹*Department of Physics, University of Adelaide, Adelaide, Australia*

²*Physics Department, SUNY Albany, Albany New York, USA*

³*Department of Physics, University of Alberta, Edmonton Alberta, Canada*

^{4a}*Department of Physics, Ankara University, Ankara, Turkey*

^{4b}*Istanbul Aydin University, Istanbul, Turkey*

^{4c}*Division of Physics, TOBB University of Economics and Technology, Ankara, Turkey*

⁵*LAPP, CNRS/IN2P3 and Université Savoie Mont Blanc, Annecy-le-Vieux, France*

⁶*High Energy Physics Division, Argonne National Laboratory, Argonne Illinois, USA*

⁷*Department of Physics, University of Arizona, Tucson Arizona, USA*

⁸*Department of Physics, The University of Texas at Arlington, Arlington Texas, USA*

⁹*Physics Department, National and Kapodistrian University of Athens, Athens, Greece*

¹⁰*Physics Department, National Technical University of Athens, Zografou, Greece*

¹¹*Department of Physics, The University of Texas at Austin, Austin Texas, USA*

¹²*Institute of Physics, Azerbaijan Academy of Sciences, Baku, Azerbaijan*

¹³*Institut de Física d'Altes Energies (IFAE), The Barcelona Institute of Science and Technology, Barcelona, Spain*

¹⁴*Institute of Physics, University of Belgrade, Belgrade, Serbia*

¹⁵*Department for Physics and Technology, University of Bergen, Bergen, Norway*

¹⁶*Physics Division, Lawrence Berkeley National Laboratory and University of California, Berkeley California, USA*

¹⁷*Department of Physics, Humboldt University, Berlin, Germany*

¹⁸*Albert Einstein Center for Fundamental Physics and Laboratory for High Energy Physics, University of Bern, Bern, Switzerland*

¹⁹*School of Physics and Astronomy, University of Birmingham, Birmingham, United Kingdom*

^{20a}*Department of Physics, Bogazici University, Istanbul, Turkey*

^{20b}*Department of Physics Engineering, Gaziantep University, Gaziantep, Turkey*

^{20d}*Istanbul Bilgi University, Faculty of Engineering and Natural Sciences, Istanbul, Turkey*

^{20c}*Bahcesehir University, Faculty of Engineering and Natural Sciences, Istanbul, Turkey*

²¹*Centro de Investigaciones, Universidad Antonio Narino, Bogota, Colombia*

^{22a}*INFN Sezione di Bologna, Italy*

^{22b}*Dipartimento di Fisica e Astronomia, Università di Bologna, Bologna, Italy*

²³*Physikalisches Institut, University of Bonn, Bonn, Germany*

²⁴*Department of Physics, Boston University, Boston Massachusetts, USA*

²⁵*Department of Physics, Brandeis University, Waltham Massachusetts, USA*

^{26a}*Universidade Federal do Rio De Janeiro COPPE/EE/IF, Rio de Janeiro, Brazil*

^{26b}*Electrical Circuits Department, Federal University of Juiz de Fora (UFJF), Juiz de Fora, Brazil*

^{26c}*Federal University of Sao Joao del Rei (UFSJ), Sao Joao del Rei, Brazil*

^{26d}*Instituto de Fisica, Universidade de Sao Paulo, Sao Paulo, Brazil*

²⁷*Physics Department, Brookhaven National Laboratory, Upton New York, USA*

^{28a}*Transilvania University of Brasov, Brasov, Romania*

^{28b}*Horia Hulubei National Institute of Physics and Nuclear Engineering, Bucharest, Romania*

^{28c}*Department of Physics, Alexandru Ioan Cuza University of Iasi, Iasi, Romania*

^{28d}*National Institute for Research and Development of Isotopic and Molecular Technologies, Physics Department, Cluj Napoca, Romania*

- ^{28e}University Politehnica Bucharest, Bucharest, Romania
^{28f}West University in Timisoara, Timisoara, Romania
- ²⁹Departamento de Física, Universidad de Buenos Aires, Buenos Aires, Argentina
³⁰Cavendish Laboratory, University of Cambridge, Cambridge, United Kingdom
³¹Department of Physics, Carleton University, Ottawa Ontario, Canada
³²CERN, Geneva, Switzerland
- ³³Enrico Fermi Institute, University of Chicago, Chicago Illinois, USA
^{34a}Departamento de Física, Pontificia Universidad Católica de Chile, Santiago, Chile
^{34b}Departamento de Física, Universidad Técnica Federico Santa María, Valparaíso, Chile
^{35a}Institute of High Energy Physics, Chinese Academy of Sciences, Beijing, China
^{35b}Department of Physics, Nanjing University, Jiangsu, China
^{35c}Physics Department, Tsinghua University, Beijing, China
- ^{36a}Department of Modern Physics and State Key Laboratory of Particle Detection and Electronics, University of Science and Technology of China, Anhui, China
^{36b}School of Physics, Shandong University, Shandong, China
^{36c}Department of Physics and Astronomy, Key Laboratory for Particle Physics, Astrophysics and Cosmology, Ministry of Education; Shanghai Key Laboratory for Particle Physics and Cosmology, Shanghai Jiao Tong University, Shanghai(also at PKU-CHEP), China
- ³⁷Université Clermont Auvergne, CNRS/IN2P3, LPC, Clermont-Ferrand, France
³⁸Nevis Laboratory, Columbia University, Irvington New York, USA
³⁹Niels Bohr Institute, University of Copenhagen, Copenhagen, Denmark
- ^{40a}INFN Gruppo Collegato di Cosenza, Laboratori Nazionali di Frascati, Italy
^{40b}Dipartimento di Fisica, Università della Calabria, Rende, Italy
- ^{41a}AGH University of Science and Technology, Faculty of Physics and Applied Computer Science, Krakow, Poland
^{41b}Marian Smoluchowski Institute of Physics, Jagiellonian University, Krakow, Poland
⁴²Institute of Nuclear Physics Polish Academy of Sciences, Krakow, Poland
⁴³Physics Department, Southern Methodist University, Dallas Texas, USA
⁴⁴Physics Department, University of Texas at Dallas, Richardson Texas, USA
⁴⁵DESY, Hamburg and Zeuthen, Germany
- ⁴⁶Lehrstuhl für Experimentelle Physik IV, Technische Universität Dortmund, Dortmund, Germany
⁴⁷Institut für Kern- und Teilchenphysik, Technische Universität Dresden, Dresden, Germany
⁴⁸Department of Physics, Duke University, Durham North Carolina, USA
- ⁴⁹SUPA - School of Physics and Astronomy, University of Edinburgh, Edinburgh, United Kingdom
⁵⁰INFN e Laboratori Nazionali di Frascati, Frascati, Italy
⁵¹Fakultät für Mathematik und Physik, Albert-Ludwigs-Universität, Freiburg, Germany
- ⁵²Departement de Physique Nucleaire et Corpusculaire, Université de Genève, Geneva, Switzerland
^{53a}INFN Sezione di Genova, Italy
^{53b}Dipartimento di Fisica, Università di Genova, Genova, Italy
- ^{54a}E. Andronikashvili Institute of Physics, Iv. Javakishvili Tbilisi State University, Tbilisi, Georgia
^{54b}High Energy Physics Institute, Tbilisi State University, Tbilisi, Georgia
⁵⁵II Physikalisches Institut, Justus-Liebig-Universität Giessen, Giessen, Germany
- ⁵⁶SUPA - School of Physics and Astronomy, University of Glasgow, Glasgow, United Kingdom
⁵⁷II Physikalisches Institut, Georg-August-Universität, Göttingen, Germany
- ⁵⁸Laboratoire de Physique Subatomique et de Cosmologie, Université Grenoble-Alpes, CNRS/IN2P3, Grenoble, France
- ⁵⁹Laboratory for Particle Physics and Cosmology, Harvard University, Cambridge Massachusetts, USA
^{60a}Kirchhoff-Institut für Physik, Ruprecht-Karls-Universität Heidelberg, Heidelberg, Germany
^{60b}Physikalisches Institut, Ruprecht-Karls-Universität Heidelberg, Heidelberg, Germany
- ^{60c}ZITI Institut für technische Informatik, Ruprecht-Karls-Universität Heidelberg, Mannheim, Germany
⁶¹Faculty of Applied Information Science, Hiroshima Institute of Technology, Hiroshima, Japan
^{62a}Department of Physics, The Chinese University of Hong Kong, Shatin, N.T., Hong Kong, China
^{62b}Department of Physics, The University of Hong Kong, Hong Kong, China
^{62c}Department of Physics and Institute for Advanced Study, The Hong Kong University of Science and Technology, Clear Water Bay, Kowloon, Hong Kong, China
- ⁶³Department of Physics, National Tsing Hua University, Taiwan, Taiwan
⁶⁴Department of Physics, Indiana University, Bloomington Indiana, USA
⁶⁵Institut für Astro- und Teilchenphysik, Leopold-Franzens-Universität, Innsbruck, Austria
⁶⁶University of Iowa, Iowa City Iowa, USA
⁶⁷Department of Physics and Astronomy, Iowa State University, Ames Iowa, USA

- ⁶⁸*Joint Institute for Nuclear Research, JINR Dubna, Dubna, Russia*
- ⁶⁹*KEK, High Energy Accelerator Research Organization, Tsukuba, Japan*
- ⁷⁰*Graduate School of Science, Kobe University, Kobe, Japan*
- ⁷¹*Faculty of Science, Kyoto University, Kyoto, Japan*
- ⁷²*Kyoto University of Education, Kyoto, Japan*
- ⁷³*Research Center for Advanced Particle Physics and Department of Physics, Kyushu University, Fukuoka, Japan*
- ⁷⁴*Instituto de Física La Plata, Universidad Nacional de La Plata and CONICET, La Plata, Argentina*
- ⁷⁵*Physics Department, Lancaster University, Lancaster, United Kingdom*
- ^{76a}*INFN Sezione di Lecce, Italy*
- ^{76b}*Dipartimento di Matematica e Fisica, Università del Salento, Lecce, Italy*
- ⁷⁷*Oliver Lodge Laboratory, University of Liverpool, Liverpool, United Kingdom*
- ⁷⁸*Department of Experimental Particle Physics, Jožef Stefan Institute and Department of Physics, University of Ljubljana, Ljubljana, Slovenia*
- ⁷⁹*School of Physics and Astronomy, Queen Mary University of London, London, United Kingdom*
- ⁸⁰*Department of Physics, Royal Holloway University of London, Surrey, United Kingdom*
- ⁸¹*Department of Physics and Astronomy, University College London, London, United Kingdom*
- ⁸²*Louisiana Tech University, Ruston Louisiana, USA*
- ⁸³*Laboratoire de Physique Nucléaire et de Hautes Energies, UPMC and Université Paris-Diderot and CNRS/IN2P3, Paris, France*
- ⁸⁴*Fysiska institutionen, Lunds universitet, Lund, Sweden*
- ⁸⁵*Departamento de Física Teórica C-15, Universidad Autónoma de Madrid, Madrid, Spain*
- ⁸⁶*Institut für Physik, Universität Mainz, Mainz, Germany*
- ⁸⁷*School of Physics and Astronomy, University of Manchester, Manchester, United Kingdom*
- ⁸⁸*CPPM, Aix-Marseille Université and CNRS/IN2P3, Marseille, France*
- ⁸⁹*Department of Physics, University of Massachusetts, Amherst Massachusetts, USA*
- ⁹⁰*Department of Physics, McGill University, Montreal Quebec, Canada*
- ⁹¹*School of Physics, University of Melbourne, Victoria, Australia*
- ⁹²*Department of Physics, The University of Michigan, Ann Arbor Michigan, USA*
- ⁹³*Department of Physics and Astronomy, Michigan State University, East Lansing Michigan, USA*
- ^{94a}*INFN Sezione di Milano, Italy*
- ^{94b}*Dipartimento di Fisica, Università di Milano, Milano, Italy*
- ⁹⁵*B.I. Stepanov Institute of Physics, National Academy of Sciences of Belarus, Minsk, Republic of Belarus*
- ⁹⁶*Research Institute for Nuclear Problems of Byelorussian State University, Minsk, Republic of Belarus*
- ⁹⁷*Group of Particle Physics, University of Montreal, Montreal Quebec, Canada*
- ⁹⁸*P.N. Lebedev Physical Institute of the Russian Academy of Sciences, Moscow, Russia*
- ⁹⁹*Institute for Theoretical and Experimental Physics (ITEP), Moscow, Russia*
- ¹⁰⁰*National Research Nuclear University MEPhI, Moscow, Russia*
- ¹⁰¹*D.V. Skobeltsyn Institute of Nuclear Physics, M.V. Lomonosov Moscow State University, Moscow, Russia*
- ¹⁰²*Fakultät für Physik, Ludwig-Maximilians-Universität München, München, Germany*
- ¹⁰³*Max-Planck-Institut für Physik (Werner-Heisenberg-Institut), München, Germany*
- ¹⁰⁴*Nagasaki Institute of Applied Science, Nagasaki, Japan*
- ¹⁰⁵*Graduate School of Science and Kobayashi-Maskawa Institute, Nagoya University, Nagoya, Japan*
- ^{106a}*INFN Sezione di Napoli, Italy*
- ^{106b}*Dipartimento di Fisica, Università di Napoli, Napoli, Italy*
- ¹⁰⁷*Department of Physics and Astronomy, University of New Mexico, Albuquerque New Mexico, USA*
- ¹⁰⁸*Institute for Mathematics, Astrophysics and Particle Physics, Radboud University Nijmegen/Nikhef, Nijmegen, Netherlands*
- ¹⁰⁹*Nikhef National Institute for Subatomic Physics and University of Amsterdam, Amsterdam, Netherlands*
- ¹¹⁰*Department of Physics, Northern Illinois University, DeKalb Illinois, USA*
- ¹¹¹*Budker Institute of Nuclear Physics, SB RAS, Novosibirsk, Russia*
- ¹¹²*Department of Physics, New York University, New York New York, USA*
- ¹¹³*Ohio State University, Columbus Ohio, USA*
- ¹¹⁴*Faculty of Science, Okayama University, Okayama, Japan*
- ¹¹⁵*Homer L. Dodge Department of Physics and Astronomy, University of Oklahoma, Norman Oklahoma, USA*
- ¹¹⁶*Department of Physics, Oklahoma State University, Stillwater Oklahoma, USA*
- ¹¹⁷*Palacký University, RCPTM, Olomouc, Czech Republic*
- ¹¹⁸*Center for High Energy Physics, University of Oregon, Eugene Oregon, USA*

- ¹¹⁹LAL, Univ. Paris-Sud, CNRS/IN2P3, Université Paris-Saclay, Orsay, France
- ¹²⁰Graduate School of Science, Osaka University, Osaka, Japan
- ¹²¹Department of Physics, University of Oslo, Oslo, Norway
- ¹²²Department of Physics, Oxford University, Oxford, United Kingdom
- ^{123a}INFN Sezione di Pavia, Italy
- ^{123b}Dipartimento di Fisica, Università di Pavia, Pavia, Italy
- ¹²⁴Department of Physics, University of Pennsylvania, Philadelphia Pennsylvania, USA
- ¹²⁵National Research Centre “Kurchatov Institute” B.P.Konstantinov Petersburg Nuclear Physics Institute, Saint Petersburg, Russia
- ^{126a}INFN Sezione di Pisa, Italy
- ^{126b}Dipartimento di Fisica E. Fermi, Università di Pisa, Pisa, Italy
- ¹²⁷Department of Physics and Astronomy, University of Pittsburgh, Pittsburgh Pennsylvania, USA
- ^{128a}Laboratório de Instrumentação e Física Experimental de Partículas - LIP, Lisboa, Portugal
- ^{128b}Faculdade de Ciências, Universidade de Lisboa, Lisboa, Portugal
- ^{128c}Department of Physics, University of Coimbra, Coimbra, Portugal
- ^{128d}Centro de Física Nuclear da Universidade de Lisboa, Lisboa, Portugal
- ^{128e}Departamento de Física, Universidade do Minho, Braga, Portugal
- ^{128f}Departamento de Física Teórica y del Cosmos and CAFPE, Universidad de Granada, Granada, Portugal
- ^{128g}Dep Física and CEFITEC of Faculdade de Ciências e Tecnologia, Universidade Nova de Lisboa, Caparica, Portugal
- ¹²⁹Institute of Physics, Academy of Sciences of the Czech Republic, Praha, Czech Republic
- ¹³⁰Czech Technical University in Prague, Praha, Czech Republic
- ¹³¹Charles University, Faculty of Mathematics and Physics, Prague, Czech Republic
- ¹³²State Research Center Institute for High Energy Physics (Protvino), NRC KI, Russia
- ¹³³Particle Physics Department, Rutherford Appleton Laboratory, Didcot, United Kingdom
- ^{134a}INFN Sezione di Roma, Italy
- ^{134b}Dipartimento di Fisica, Sapienza Università di Roma, Roma, Italy
- ^{135a}INFN Sezione di Roma Tor Vergata, Italy
- ^{135b}Dipartimento di Fisica, Università di Roma Tor Vergata, Roma, Italy
- ^{136a}INFN Sezione di Roma Tre, Italy
- ^{136b}Dipartimento di Matematica e Fisica, Università Roma Tre, Roma, Italy
- ^{137a}Faculté des Sciences Ain Chock, Réseau Universitaire de Physique des Hautes Energies - Université Hassan II, Casablanca, Morocco
- ^{137b}Centre National de l’Energie des Sciences Techniques Nucleaires, Rabat, Morocco
- ^{137c}Faculté des Sciences Semlalia, Université Cadi Ayyad, LPHEA-Marrakech, Morocco
- ^{137d}Faculté des Sciences, Université Mohamed Premier and LPTPM, Oujda, Morocco
- ^{137e}Faculté des sciences, Université Mohammed V, Rabat, Morocco
- ¹³⁸DSM/IRFU (Institut de Recherches sur les Lois Fondamentales de l’Univers), CEA Saclay (Commissariat à l’Energie Atomique et aux Energies Alternatives), Gif-sur-Yvette, France
- ¹³⁹Santa Cruz Institute for Particle Physics, University of California Santa Cruz, Santa Cruz California, USA
- ¹⁴⁰Department of Physics, University of Washington, Seattle Washington, USA
- ¹⁴¹Department of Physics and Astronomy, University of Sheffield, Sheffield, United Kingdom
- ¹⁴²Department of Physics, Shinshu University, Nagano, Japan
- ¹⁴³Department Physik, Universität Siegen, Siegen, Germany
- ¹⁴⁴Department of Physics, Simon Fraser University, Burnaby British Columbia, Canada
- ¹⁴⁵SLAC National Accelerator Laboratory, Stanford California, USA
- ^{146a}Faculty of Mathematics, Physics & Informatics, Comenius University, Bratislava, Slovak Republic
- ^{146b}Department of Subnuclear Physics, Institute of Experimental Physics of the Slovak Academy of Sciences, Kosice, Slovak Republic
- ^{147a}Department of Physics, University of Cape Town, Cape Town, South Africa
- ^{147b}Department of Physics, University of Johannesburg, Johannesburg, South Africa
- ^{147c}School of Physics, University of the Witwatersrand, Johannesburg, South Africa
- ^{148a}Department of Physics, Stockholm University, Sweden
- ^{148b}The Oskar Klein Centre, Stockholm, Sweden
- ¹⁴⁹Physics Department, Royal Institute of Technology, Stockholm, Sweden
- ¹⁵⁰Departments of Physics & Astronomy and Chemistry, Stony Brook University, Stony Brook New York, USA
- ¹⁵¹Department of Physics and Astronomy, University of Sussex, Brighton, United Kingdom

- ¹⁵²*School of Physics, University of Sydney, Sydney, Australia*
¹⁵³*Institute of Physics, Academia Sinica, Taipei, Taiwan*
¹⁵⁴*Department of Physics, Technion: Israel Institute of Technology, Haifa, Israel*
¹⁵⁵*Raymond and Beverly Sackler School of Physics and Astronomy, Tel Aviv University, Tel Aviv, Israel*
¹⁵⁶*Department of Physics, Aristotle University of Thessaloniki, Thessaloniki, Greece*
¹⁵⁷*International Center for Elementary Particle Physics and Department of Physics, The University of Tokyo, Tokyo, Japan*
¹⁵⁸*Graduate School of Science and Technology, Tokyo Metropolitan University, Tokyo, Japan*
¹⁵⁹*Department of Physics, Tokyo Institute of Technology, Tokyo, Japan*
¹⁶⁰*Tomsk State University, Tomsk, Russia*
¹⁶¹*Department of Physics, University of Toronto, Toronto Ontario, Canada*
^{162a}*INFN-TIFPA, Italy*
^{162b}*University of Trento, Trento, Italy*
^{163a}*TRIUMF, Vancouver British Columbia, Canada*
^{163b}*Department of Physics and Astronomy, York University, Toronto Ontario, Canada*
¹⁶⁴*Faculty of Pure and Applied Sciences, and Center for Integrated Research in Fundamental Science and Engineering, University of Tsukuba, Tsukuba, Japan*
¹⁶⁵*Department of Physics and Astronomy, Tufts University, Medford Massachusetts, USA*
¹⁶⁶*Department of Physics and Astronomy, University of California Irvine, Irvine California, USA*
^{167a}*INFN Gruppo Collegato di Udine, Sezione di Trieste, Udine, Italy*
^{167b}*ICTP, Trieste, Italy*
^{167c}*Dipartimento di Chimica, Fisica e Ambiente, Università di Udine, Udine, Italy*
¹⁶⁸*Department of Physics and Astronomy, University of Uppsala, Uppsala, Sweden*
¹⁶⁹*Department of Physics, University of Illinois, Urbana Illinois, USA*
¹⁷⁰*Instituto de Fisica Corpuscular (IFIC), Centro Mixto Universidad de Valencia - CSIC, Spain*
¹⁷¹*Department of Physics, University of British Columbia, Vancouver British Columbia, Canada*
¹⁷²*Department of Physics and Astronomy, University of Victoria, Victoria British Columbia, Canada*
¹⁷³*Department of Physics, University of Warwick, Coventry, United Kingdom*
¹⁷⁴*Waseda University, Tokyo, Japan*
¹⁷⁵*Department of Particle Physics, The Weizmann Institute of Science, Rehovot, Israel*
¹⁷⁶*Department of Physics, University of Wisconsin, Madison Wisconsin, USA*
¹⁷⁷*Fakultät für Physik und Astronomie, Julius-Maximilians-Universität, Würzburg, Germany*
¹⁷⁸*Fakultät für Mathematik und Naturwissenschaften, Fachgruppe Physik, Bergische Universität Wuppertal, Wuppertal, Germany*
¹⁷⁹*Department of Physics, Yale University, New Haven Connecticut, USA*
¹⁸⁰*Yerevan Physics Institute, Yerevan, Armenia*
¹⁸¹*CH-1211 Geneva 23, Switzerland*
¹⁸²*Centre de Calcul de l'Institut National de Physique Nucléaire et de Physique des Particules (IN2P3), Villeurbanne, France*
¹⁸³*Academia Sinica Grid Computing, Institute of Physics, Academia Sinica, Taipei, Taiwan*

^aDeceased.

^bAlso at Department of Physics, King's College London, London, United Kingdom.

^cAlso at Institute of Physics, Azerbaijan Academy of Sciences, Baku, Azerbaijan.

^dAlso at Novosibirsk State University, Novosibirsk, Russia.

^eAlso at TRIUMF, Vancouver British Columbia, Canada.

^fAlso at Department of Physics & Astronomy, University of Louisville, Louisville, Kentucky, USA.

^gAlso at Physics Department, An-Najah National University, Nablus, Palestine.

^hAlso at Department of Physics, California State University, Fresno California, USA.

ⁱAlso at Department of Physics, University of Fribourg, Fribourg, Switzerland.

^jAlso at II Physikalisches Institut, Georg-August-Universität, Göttingen, Germany.

^kAlso at Departament de Física de la Universitat Autònoma de Barcelona, Barcelona, Spain.

^lAlso at Departamento de Física e Astronomia, Faculdade de Ciências, Universidade do Porto, Portugal.

^mAlso at Tomsk State University, Tomsk, Russia.

ⁿAlso at The Collaborative Innovation Center of Quantum Matter (CICQM), Beijing, China.

^oAlso at Università di Napoli Parthenope, Napoli, Italy.

^pAlso at Institute of Particle Physics (IPP), Canada.

^qAlso at Horia Hulubei National Institute of Physics and Nuclear Engineering, Bucharest, Romania.

^rAlso at Department of Physics, St. Petersburg State Polytechnical University, St. Petersburg, Russia.

^sAlso at Borough of Manhattan Community College, City University of New York, New York City, USA.

^t Also at Centre for High Performance Computing, CSIR Campus, Rosebank, Cape Town, South Africa.

^u Also at Louisiana Tech University, Ruston Louisiana, USA.

^v Also at Institutio Catalana de Recerca i Estudis Avancats, ICREA, Barcelona, Spain.

^w Also at Graduate School of Science, Osaka University, Osaka, Japan.

^x Also at Fakultät für Mathematik und Physik, Albert-Ludwigs-Universität, Freiburg, Germany.

^y Also at Institute for Mathematics, Astrophysics and Particle Physics, Radboud University Nijmegen/Nikhef, Nijmegen, Netherlands.

^z Also at Department of Physics, The University of Texas at Austin, Austin Texas, USA.

^{aa} Also at Institute of Theoretical Physics, Ilia State University, Tbilisi, Georgia.

^{bb} Also at CERN, Geneva, Switzerland.

^{cc} Also at Georgian Technical University (GTU), Tbilisi, Georgia.

^{dd} Also at Ochadai Academic Production, Ochanomizu University, Tokyo, Japan.

^{ee} Also at Manhattan College, New York New York, USA.

^{ff} Also at Departamento de Física, Pontificia Universidad Católica de Chile, Santiago, Chile.

^{gg} Also at Department of Physics, The University of Michigan, Ann Arbor Michigan, USA.

^{hh} Also at School of Physics, Shandong University, Shandong, China.

ⁱⁱ Also at Departamento de Física Teórica y del Cosmos and CAFPE, Universidad de Granada, Granada, Portugal.

^{jj} Also at Department of Physics, California State University, Sacramento California, USA.

^{kk} Also at Moscow Institute of Physics and Technology State University, Dolgoprudny, Russia.

^{ll} Also at Departement de Physique Nucleaire et Corpusculaire, Université de Genève, Geneva, Switzerland.

^{mm} Also at Institut de Física d'Altes Energies (IFAE), The Barcelona Institute of Science and Technology, Barcelona, Spain.

ⁿⁿ Also at School of Physics, Sun Yat-sen University, Guangzhou, China.

^{oo} Also at Institute for Nuclear Research and Nuclear Energy (INRNE) of the Bulgarian Academy of Sciences, Sofia, Bulgaria.

^{pp} Also at Faculty of Physics, M.V.Lomonosov Moscow State University, Moscow, Russia.

^{qq} Also at National Research Nuclear University MEPHI, Moscow, Russia.

^{rr} Also at Department of Physics, Stanford University, Stanford California, USA.

^{ss} Also at Institute for Particle and Nuclear Physics, Wigner Research Centre for Physics, Budapest, Hungary.

^{tt} Also at Giresun University, Faculty of Engineering, Turkey.

^{uu} Also at CPPM, Aix-Marseille Université and CNRS/IN2P3, Marseille, France.

^{vv} Also at Department of Physics, Nanjing University, Jiangsu, China.

^{ww} Also at University of Malaya, Department of Physics, Kuala Lumpur, Malaysia.

^{xx} Also at Institute of Physics, Academia Sinica, Taipei, Taiwan.

^{yy} Also at LAL, Univ. Paris-Sud, CNRS/IN2P3, Université Paris-Saclay, Orsay, France.